

# Mono- and Dinuclear Titanium(III)/Titanium(IV) Complexes with 1,4,7-Trimethyl-1,4,7-triazacyclononane (L). Crystal Structures of a Compositionally Disordered Green and a Blue Form of [LTiCl<sub>3</sub>]. Structures of [LTi(O)(NCS)<sub>2</sub>], [LTi(OCH<sub>3</sub>)Br<sub>2</sub>](ClO<sub>4</sub>), and [L<sub>2</sub>Ti<sub>2</sub>(O)<sub>2</sub>F<sub>2</sub>(μ-F)](PF<sub>6</sub>)

Axel Bodner,<sup>1a</sup> Peter Jeske,<sup>1a</sup> Thomas Weyhermüller,<sup>1a</sup> Karl Wiegardt,<sup>\*,1a</sup> Erich Dubler,<sup>1b</sup> Helmut Schmalle,<sup>1b</sup> and Bernhard Nuber<sup>1c</sup>

Lehrstuhl für Anorganische Chemie I, Ruhr-Universität, D-4630 Bochum, Germany, Institut für Anorganische Chemie der Universität, CH-8057 Zürich, Switzerland, and Anorganische-Chemisches Institut der Universität, D-6900 Heidelberg, Germany

Received February 5, 1992

The coordination chemistry of titanium(III) and -(IV) with the macrocycle 1,4,7-trimethyl-1,4,7-triazacyclononane (L, C<sub>9</sub>H<sub>21</sub>N<sub>3</sub>) has been investigated. Reaction of TiCl<sub>3</sub> with L in CH<sub>3</sub>CN at 20 °C affords blue [LTiCl<sub>3</sub>] (1) whereas at elevated temperature green crystals (1a) were obtained. 1a is shown to consist of compositionally disordered crystals containing [LTi<sup>III</sup>Cl<sub>3</sub>] and probably an [LTi<sup>IV</sup>(O)Cl<sub>2</sub>] impurity. The crystal structures of 1 and 1a have been determined. Crystal data for 1 and, in brackets, for 1a: space group *P*2<sub>1</sub>/*c* (*P*2<sub>1</sub>/*c*), *a* = 12.365 (5) Å (12.430 (8) Å), *b* = 7.348 (2) Å, (7.337 (3) Å), *c* = 15.897 (3) Å (15.929 (5) Å), β = 90.06 (2)° (90.19 (3)°), *V* = 1443 (1) Å<sup>3</sup> (1453 (2) Å<sup>3</sup>) *Z* = 4 (4). It has been possible to detect the impurity in 1a by comparing the temperature parameters of the Cl atoms and the residual electron density maps of the final difference Fourier calculations of 1 and 1a. The structure of the [LTi<sup>III</sup>Cl<sub>3</sub>] molecule is identical in both 1 and 1a; only slight differences of the packing are observed. Implications of this observation on the “distortional” or “bond stretch” isomerism phenomenon are discussed. Reaction of TiBr<sub>4</sub> with L in CH<sub>3</sub>CN yields [LTiBr<sub>3</sub>] (2) whereas TiCl<sub>4</sub> reacts with L at 20 °C affording [LTiCl<sub>3</sub>]Cl (5). Complex 1 reacts with CF<sub>3</sub>SO<sub>3</sub>H to give blue [LTi(O<sub>3</sub>SCF<sub>3</sub>)<sub>3</sub>] (3) which is a good starting material for the synthesis of complexes containing the LTi<sup>III</sup> fragment. Thus 3 reacts with NaSCN in CH<sub>3</sub>OH to give [LTi<sup>III</sup>(NCS)<sub>3</sub>] (4). Oxidation of 1 by azide yields [LTiCl<sub>2</sub>(N<sub>3</sub>)] [BPh<sub>4</sub>] (6) whereas oxidation of 4 by O<sub>2</sub> in the presence of water gives [LTi<sup>IV</sup>(O)(NCS)<sub>2</sub>] (7). Crystal data for 7: space group *Pna*2<sub>1</sub>, *a* = 7.076 (2) Å, *b* = 14.247 (3) Å, *c* = 16.163 (5) Å, *V* = 1629 (2) Å<sup>3</sup>, *Z* = 4. Complex 7 is the first structurally characterized octahedral complex of titanium(IV) containing a terminal oxo ligand (titanyl group): Ti=O 1.638 (3) Å. Air oxidation of 2 in methanol yields [LTi<sup>IV</sup>(OCH<sub>3</sub>)Br<sub>2</sub>](ClO<sub>4</sub>) (8). Crystal data for 8: space group *Pnma*, *a* = 12.819 (3) Å, *b* = 11.608 (2) Å, *c* = 12.686 (3) Å, *V* = 1888 (1) Å<sup>3</sup>, *Z* = 4. TiCl<sub>3</sub> and the ligand L in water containing dimethylformamide form the μ-oxo-bridged dinuclear species [L<sub>2</sub>Ti<sup>III</sup><sub>2</sub>Cl<sub>4</sub>(μ-O)] (9) which is oxidized by air to the mixed-valence species [L<sub>2</sub>Ti<sub>2</sub>Cl<sub>4</sub>(μ-O)]Cl·2H<sub>2</sub>O (10) and, finally, to [L<sub>2</sub>Ti<sup>IV</sup><sub>2</sub>Cl<sub>4</sub>(μ-O)]Cl<sub>2</sub>·2.5H<sub>2</sub>O (11). Complete hydrolysis and air oxidation of 1 in water at pH 7 (NaHCO<sub>3</sub>) yields colorless crystals of [L<sub>2</sub>Ti<sup>IV</sup><sub>2</sub>(O)<sub>2</sub>(OH)<sub>2</sub>(μ-O)]·8H<sub>2</sub>O (12). When the hydrolysis/oxidation reaction of 1 is carried out in a water/nitromethane mixture in the presence of NaF, yellow crystals of [L<sub>2</sub>Ti<sub>2</sub>F<sub>2</sub>(O)<sub>2</sub>(μ-F)](PF<sub>6</sub>) (13) were obtained. Crystal data for 13: space group *P* $\bar{1}$ , *a* = 7.676 (5) Å, *b* = 7.695 (6) Å, *c* = 13.67 (1) Å, α = 75.05 (6)°, β = 79.67 (6)°, γ = 70.03 (6)°, *V* = 729 (1) Å<sup>3</sup>, *Z* = 1.

## Introduction

In this paper we describe some preparative and structural coordination chemistry of the tridentate facially coordinating macrocycle 1,4,7-trimethyl-1,4,7-triazacyclononane (L)<sup>2</sup> with titanium(III) and -(IV). Due to the inherent lability of Ti–N bonds toward hydrolysis and the greater thermodynamic stability of Ti–O bonds, only relatively few titanium complexes with amine ligands have been characterized.<sup>3</sup> [(N<sub>4</sub>C<sub>12</sub>H<sub>25</sub>)<sub>2</sub>Ti<sub>2</sub>(μ-O)] ((N<sub>4</sub>C<sub>12</sub>H<sub>25</sub>)<sub>3</sub>)<sup>3-</sup> = trianion of 1,5,9,13-tetraazacyclohexadecane,<sup>4a</sup> [Ti(C<sub>22</sub>H<sub>22</sub>N<sub>4</sub>)Cl<sub>2</sub>],<sup>4c</sup> and [L'<sub>4</sub>Ti<sub>4</sub>(μ-O)<sub>6</sub>]<sup>4+</sup> 4b (L' = 1,4,7-triazacyclononane) have been reported; they are the first examples of structurally characterized titanium(IV) complexes containing macrocyclic amine ligands.

During the course of the present investigation we made a serendipitous discovery which bears relevance to the possibility of an experimental verification of so-called “distortional”<sup>5–8</sup> or “bond stretch”<sup>9,10</sup> isomers by X-ray crystallography.<sup>11,12</sup> It was found that the reaction between L and TiCl<sub>3</sub> in acetonitrile at room temperature under anaerobic conditions produced nice blue crystals of [LTi<sup>III</sup>Cl<sub>3</sub>]. When the reaction was carried out with heating to reflux under otherwise identical conditions, green crystals which apparently also analyzed as [LTi<sup>III</sup>Cl<sub>3</sub>] were obtained.

- (1) (a) Ruhr-Universität Bochum. (b) Universität Zürich. (c) Universität Heidelberg.  
 (2) (a) Wiegardt, K.; Chaudhuri, P.; *Progress in Inorganic Chemistry*; Lippard, S. J., Ed.; Wiley: New York, 1988; Vol. 35, p 329. (b) Bhula, R.; Osvath, P.; Weatherburn, D. C. *Coord. Chem. Rev.* 1988, 91, 89.  
 (3) McAuliffe, C. A.; Barrat, D. S. *Comprehensive Coordination Chemistry*; Wilkinson, G., Gillard, R. D., McCleverty, J. A., Eds.; Pergamon Press: Oxford, England, 1987; Vol. 3, p 323.  
 (4) (a) Olmstead, M. M.; Power, P. P.; Viggiano, M. *J. Am. Chem. Soc.* 1983, 105, 2927. (b) Wiegardt, K.; Ventur, D.; Tsay, Y. H.; Krüger, C. *Inorg. Chim. Acta* 1985, 99, L25. (c) Goedken, V. L.; Ladd, J. A. *J. Chem. Soc., Chem. Commun.* 1982, 142.

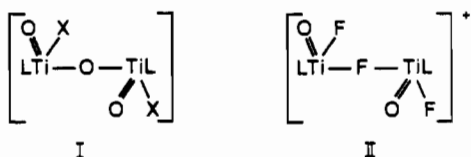
- (5) (a) Chatt, J.; Manojlovic-Muir, L.; Muir, K. W. *J. Chem. Soc. D* 1971, 655. (b) Butcher, A. V.; Chatt, J. *J. Chem. Soc. A* 1970, 2652.  
 (6) (a) Backes-Dahmann, G.; Wiegardt, K.; Nuber, B.; Weiss, J. *Angew. Chem., Int. Ed. Engl.* 1985, 24, 777. (b) Backes-Dahmann, G.; Wiegardt, K. *Inorg. Chem.* 1985, 24, 4044.  
 (7) (a) Bashall, A.; McPartlin, M. *Acta Crystallogr.* 1990, 46A, C-221. (b) Bashall, A.; Gibson, V. C.; Kee, T. P.; McPartlin, M.; Robinson, O. B.; Shaw, A. *Angew. Chem., Int. Ed. Engl.* 1991, 30, 982.  
 (8) Degnan, I. A.; Behm, J.; Cook, M. R.; Herrmann, W. A. *Inorg. Chem.* 1991, 30, 2165.  
 (9) Yves, J.; Lledos, A.; Burdett, J. K.; Hoffmann, R. *J. Am. Chem. Soc.* 1988, 110, 4506.  
 (10) Song, J.; Hall, M. B. *Inorg. Chem.* 1991, 30, 4433.  
 (11) Yoon, K.; Parkin, G.; Rheingold, A. L. *J. Am. Chem. Soc.* 1991, 113, 1437.  
 (12) Desroches, P. J.; Nebesny, K. W.; LaBarre, M. J.; Lincoln, S. E.; Loehr, T. M.; Enemark, J. H. *J. Am. Chem. Soc.* 1991, 113, 9193.

Careful spectroscopic analysis of this green material led to the conclusion that the green crystals are compositionally disordered by ca. 10% with presumably  $[\text{LTi}^{\text{IV}}(\text{O})\text{Cl}_2]$ . To our amazement, high-quality X-ray structure determinations of both a blue and a green crystal revealed only a weak indication of an impurity in the latter.

Since the octahedral species  $[\text{LTi}(\text{O})\text{Cl}_2]$  containing a Ti=O group (titanyl group) is the presumed impurity, we have studied the hydrolysis reaction of  $[\text{LTiCl}_3]$  under anaerobic and oxidative conditions in an attempt to isolate a pure sample of  $[\text{LTi}(\text{O})\text{Cl}_2]$ . The resulting dinuclear oxo-bridged complexes are described here. Some aspects of this work have been communicated previously.<sup>13</sup>

Structurally characterized octahedral titanyl complexes are unknown to date due to the propensity of oxotitanium(IV) complexes to form bridges of the type Ti–O–Ti.<sup>3</sup> Only a few titanyl complexes where the Ti(IV) ion is five-<sup>14–18</sup> or seven-coordinate<sup>19</sup> have been structurally characterized. The existence of such species in solution has been implied by infrared, Raman,<sup>20</sup> and <sup>17</sup>O NMR spectroscopy.<sup>21</sup> Although we have not been able to prepare  $[\text{LTi}(\text{O})\text{Cl}_2]$ , we succeeded in synthesizing its closely related analogue  $[\text{LTi}(\text{O})(\text{NCS})_2]$ .

Finally, we have synthesized two dinuclear titanium(IV) complexes which in addition to an oxo or fluoride bridging group contain terminal oxo groups, (Ti=O). Complexes of type I are very common for the higher oxidation states of vanadium, molybdenum, tungsten, and rhenium but were not known for titanium.



## Experimental Section

**Reagents.** The ligand 1,4,7-trimethyl-1,4,7-triazacyclononane (L) was prepared according to a published procedure.<sup>22</sup> The solvent acetonitrile was purchased from Baker ( $[\text{H}_2\text{O}] \approx 0.1\%$ ) and was used as received.

**$[\text{LTiCl}_3]$  (Blue) (1).** An argon-purged mixture of  $\text{TiCl}_3$  (1.0 g, 6.5 mmol) in acetonitrile (25 mL) was heated to reflux for 30 min. After the suspension was allowed to cool to room temperature, a solution of 1,4,7-trimethyl-1,4,7-triazacyclononane (1.2 g, 7.0 mmol) in acetonitrile (10 mL) was added dropwise. The mixture was stirred at 20 °C for 30 min under an argon blanketing atmosphere. A blue solid precipitated which was collected by filtration, washed with dry diethyl ether, and air-dried. Yield: 2.0 g; 92%. The product is stable for weeks in dry air. Anal. Calcd for  $\text{C}_9\text{H}_{21}\text{N}_3\text{Cl}_3\text{Ti}$ : C, 33.2; H, 6.5; N, 12.9; Cl, 32.6; Ti, 14.8. Found: C, 33.8; H, 6.7; N, 12.9; Cl, 32.4; Ti, 15.1.

**$[\text{LTiCl}_3]$  (Green) (1a). Method A.** When the above reaction between the blue solution and the ligand L was carried out with heating to reflux under anaerobic conditions (argon blanketing atmosphere) a green precipitate formed immediately. Yield: 1.7 g. It was found that the color of this material varied from blue-green to light green depending on the amount of water in the solvent acetonitrile ( $\approx 2\text{--}5\%$ ) and probably on the adventitious presence of oxygen. The less of each present the more bluish was the product obtained.

**Method B.** A deoxygenated acetonitrile solution (20 mL) of  $\text{TiCl}_4$  (1.0 g, 5.3 mmol) was heated to reflux until a clear, green solution was obtained. To this solution was added L (1.50 g, 8.6 mmol). Upon cooling to room temperature, a green precipitate formed which was collected by filtration, washed with diethyl ether, and air-dried. Yield: 1.50 g (87%). Anal. Calcd for  $\text{C}_9\text{H}_{21}\text{N}_3\text{Cl}_3\text{Ti}$ : C, 33.2; H, 6.5; N, 12.9; Cl, 32.6. Found: C, 32.8; H, 6.6; N, 12.6; Cl, 32.15.

**$[\text{LTiBr}_3]$  (2).** A solution of  $\text{TiBr}_4$  (5.0 g, 13.6 mmol) in acetonitrile (40 mL) was heated to reflux under an argon atmosphere. The resulting dark red solution was cooled to 20 °C whereupon a red precipitate formed. To this mixture was added dropwise a solution of L (2.5 g, 14.3 mmol) in  $\text{CH}_3\text{CN}$  (10 mL) at ambient temperature. After stirring for 1 h, deoxygenated water (20 mL) was added which initiated the precipitation of a green microcrystalline solid which was collected by filtration, washed with deoxygenated  $\text{CH}_3\text{CN}$  and diethyl ether, and dried in vacuo. The solid is stable in air and not hygroscopic. Yield: 2.2 g (35% with respect to  $\text{TiBr}_4$ ). Anal. Calcd for  $\text{C}_9\text{H}_{21}\text{N}_3\text{Br}_3\text{Ti}$ : C, 23.5; H, 4.6; N, 9.1. Found: C, 23.7; H, 4.4; N, 8.9.

**$[\text{LTi}(\text{O}_3\text{SCF}_3)_3]$  (3).** To  $\text{LTiCl}_3$  (1) (0.5 g, 1.5 mmol) under an argon atmosphere was added dropwise with efficient cooling ( $-5$  °C) trifluoromethanesulfonic acid (3 mL). A green solution formed with concomitant generation of gaseous HCl. Addition of deoxygenated dry diethyl ether initiated the precipitation of a blue solid material which was collected by filtration under argon and washed with dry ether. The product is very hygroscopic and air-sensitive. Yield: 0.90 g (90%). Anal. Calcd for  $\text{C}_{12}\text{H}_{21}\text{F}_9\text{O}_9\text{S}_3\text{Ti}$ : C, 21.6; H, 3.2; N, 6.3. Found: C, 21.6; H, 3.2; N, 6.1.

**$[\text{LTi}(\text{NCS})_3]$  (4).** To a deoxygenated solution of NaSCN (1.0 g, 12.3 mmol) in methanol (15 mL) was added 3 (0.40 g, 0.60 mmol). After stirring for 30 min at 20 °C a blue microcrystalline solid precipitated which was collected by filtration, washed with deoxygenated diethyl ether, and dried in vacuo. The product is very moisture and air-sensitive. Yield: 0.16 g (67%). Anal. Calcd for  $\text{C}_{12}\text{H}_{21}\text{N}_6\text{S}_3\text{Ti}$ : C, 36.6; H, 5.4; N, 21.4. Found: C, 36.4; H, 5.3; N, 20.9.

**$[\text{LTiCl}_3]\text{Cl}$  (5).** A solution of  $\text{TiCl}_4$  (0.50 g, 2.6 mmol) in dry acetonitrile (25 mL) was stirred at 20 °C for 30 min after which time L (0.80 g, 4.7 mmol) was added. Addition of dry diethyl ether (50 mL) to the brown solution initiated the precipitation of a pale yellow solid which was collected by filtration, washed with dry diethyl ether, and air-dried. The product is stable in air and not particularly sensitive to moisture. Yield: 0.40 g (43%). Anal. Calcd for  $\text{C}_9\text{H}_{21}\text{N}_3\text{Cl}_4\text{Ti}$ : C, 29.95; H, 5.8; N, 11.6; Cl, 39.2; Ti, 13.3. Found: C, 30.1; H, 6.1; N, 11.5; Cl, 38.9; Ti, 13.5.

**$[\text{LTiCl}_2(\text{N}_3)]\text{[BPh}_4]$  (6).** To a solution of  $\text{NaN}_3$  (0.50 g, 8.0 mmol) in methanol (20 mL) was added 1 (0.30 g, 1.0 mmol). This mixture was heated to reflux for 10 min. After cooling to ambient temperature sodium tetraphenylborate (0.50 g) was added whereupon a colorless precipitate formed, which was collected by filtration, washed with cold diethyl ether, and air-dried. Yield: 0.30 g (45%). Anal. Calcd for  $\text{C}_{33}\text{H}_{41}\text{N}_6\text{BCl}_2\text{Ti}$ : C, 60.8; H, 6.3; N, 12.9; Ti, 7.4. Found: C, 61.1; H, 6.0; N, 12.8; Ti, 7.2.

**$[\text{LTiO}(\text{NCS})_2]$  (7).** A solution of 4 (1.0 g, 2.5 mmol) in acetonitrile (40 mL) was heated to 55 °C in the presence of air until the purple color had disappeared and a yellow solution was obtained (ca. 1.5 h). This solution was allowed to stand in an open vessel for 48 h after which time a pale yellow microcrystalline solid formed (0.45 g). This material was recrystallized from an acetonitrile/water mixture (4:1, 50 mL). Anal. Calcd for  $\text{C}_{12}\text{H}_{21}\text{N}_5\text{S}_2\text{OTi}$ : C, 37.6; H, 6.0; N, 19.9. Found: C, 37.4; H, 5.9; N, 19.8.

**$[\text{LTi}(\text{OCH}_3)_2\text{Br}_2](\text{ClO}_4)$  (8).** A mixture of 2 (0.46 g, 1.0 mmol) in methanol (10 mL) and acetonitrile (10 mL) was heated to 60 °C in the presence of air until a clear yellow-orange solution was obtained. Addition of solid  $\text{NaClO}_4$  (0.20 g) initiated the precipitation of a yellow microcrystalline solid (0.20 g, 39%) within 1 week. Single crystals suitable for an X-ray structure determination were obtained by recrystallization from a 1:1 methanol/acetonitrile mixture. <sup>1</sup>H NMR (80 MHz,  $\text{CD}_3\text{CN}$ ,  $\delta$ , ppm): 2.95 (s, 6 H), two magnetically equivalent  $\text{CH}_3$  groups (C5 and C5a in Figure 13); 3.40 (s, 3 H),  $\text{CH}_3$  group (C1, Figure 13); 2.75–3.90 (m, 12 H), methylene groups; 4.80 (s, 3 H),  $\text{OCH}_3$  group (C6, Figure 13). Anal. Calcd for  $\text{C}_{10}\text{H}_{24}\text{N}_3\text{Br}_2\text{ClO}_4\text{Ti}$ : C, 23.6; H, 4.7; N, 8.3;  $\text{ClO}_4$ , 19.4. Found: C, 23.8; H, 4.9; N, 8.3;  $\text{ClO}_4$ , 19.3.

**$[\text{L}_2\text{Ti}_2(\mu\text{-O})\text{Cl}_4]$  (9).** To an argon-purged solution of L (0.80 g, 4.6 mmol) in dimethylformamide (dmf) (25 mL) which contained ca. 2% water was added  $\text{TiCl}_3$  (0.50 g, 3.2 mmol). The mixture was heated to reflux for 30 min under an argon atmosphere. Upon cooling to room temperature, a blue precipitate formed which was collected by filtration, washed three times with hot deoxygenated  $\text{CH}_2\text{Cl}_2$  and diethyl ether, and air-dried. Yield: 0.45 g (24%). Anal. Calcd for  $\text{C}_{18}\text{H}_{42}\text{N}_6\text{OCl}_4\text{Ti}_2$ : C,

- (13) Bodner, A.; Della Vedova, S. P. C.; Wieghardt, K.; Nuber, B.; Weiss, J. *J. Chem. Soc., Chem. Commun.* **1990**, 1042.  
 (14) Guillard, R.; Latour, J. M.; Lecomte, C.; Marchon, J.-C.; Protas, J.; Ripoll, D. *Inorg. Chem.* **1978**, *17*, 1228.  
 (15) Dwyer, P. N.; Puppe, L.; Buchler, J. W.; Scheidt, W. R. *Inorg. Chem.* **1975**, *14*, 1782.  
 (16) Hiller, W.; Strähle, J.; Kobel, W.; Hanack, M. *Z. Kristallogr.* **1982**, *159*, 173.  
 (17) Feltz, A. *Z. Chem.* **1967**, *7*, 158.  
 (18) Dehnicke, K.; Pausewang, G.; Rüdorff, W. *Z. Anorg. Allg. Chem.* **1969**, *366*, 64.  
 (19) Peng-Ju, L.; Sheng-Hua, H.; Kun-Yao, H.; Ru-Ji, W.; Mak, C. W. *Inorg. Chim. Acta* **1990**, *175*, 105.  
 (20) Grätzel, M.; Rotzinger, F. P. *Inorg. Chem.* **1985**, *24*, 2320.  
 (21) Comba, P.; Merbach, A. *Inorg. Chem.* **1987**, *27*, 1315.  
 (22) Wieghardt, K.; Chaudhuri, P.; Nuber, B.; Weiss, J. *Inorg. Chem.* **1982**, *21*, 3086.

Table I. Crystallographic Data of Complexes

	blue 1	green 1a	7	8	13
chem formula	C <sub>9</sub> H <sub>21</sub> N <sub>3</sub> Cl <sub>3</sub> Ti	C <sub>9</sub> H <sub>21</sub> N <sub>3</sub> Cl <sub>3</sub> Ti	C <sub>12</sub> H <sub>21</sub> N <sub>3</sub> S <sub>2</sub> O <sub>2</sub> Ti	C <sub>10</sub> H <sub>24</sub> N <sub>3</sub> Br <sub>2</sub> ClO <sub>5</sub> Ti	C <sub>18</sub> H <sub>42</sub> N <sub>6</sub> O <sub>2</sub> F <sub>9</sub> PTi <sub>2</sub>
fw	325.55	325.55	351.35	509.5	672.36
space group	<i>P2<sub>1</sub>/c</i>	<i>P2<sub>1</sub>/c</i>	<i>Pna2<sub>1</sub></i>	<i>Pnma</i>	<i>P1</i>
<i>a</i> , Å	12.356 (5)	12.430 (8)	7.076 (2)	12.819 (3)	7.676 (6)
<i>b</i> , Å	7.348 (2)	7.337 (3)	14.247 (3)	11.608 (2)	7.695 (6)
<i>c</i> , Å	15.897 (3)	15.929 (5)	16.163 (5)	12.686 (3)	13.67 (1)
$\alpha$ , deg					75.05 (6)
$\beta$ , deg	90.06 (2)	90.19 (3)			79.67 (6)
$\gamma$ , deg					70.03 (6)
<i>V</i> , Å <sup>3</sup>	1443 (1)	1453 (2)	1629 (2)	1888 (1)	730 (1)
<i>Z</i>	4	4	4	4	1
<i>T</i> , K	295	295	295	295	295
radiation $\lambda$ , Å	0.710 73	0.710 73	0.071 73	0.710 73	0.710 73
$\rho_{\text{calcd}}$ , g·cm <sup>-3</sup>	1.50	1.49	1.43	1.793	1.53
$\mu$ (Mo K $\alpha$ ), cm <sup>-1</sup>	10.68	10.61	7.7	48.1	6.8
transm coeff	0.633–0.723	0.677–0.743	0.86–1.00	0.011–0.030	0.835–0.953
<i>R</i> <sup>a</sup>	0.050	0.043	0.050	0.061	0.080
<i>R</i> <sub>w</sub> <sup>b</sup>	0.057	0.046	0.047	0.056	0.082

<sup>a</sup>  $R = \sum ||F_o| - |F_c|| / \sum |F_o|$ . <sup>b</sup>  $R_w = \{ \sum w(|F_o| - |F_c|)^2 / \sum w|F_o|^2 \}^{1/2}$ .

36.0; H, 6.9; N, 13.8; Cl, 24.4; Ti, 15.9. Found: C, 36.2; H, 7.1; N, 14.0; Cl, 24.0; Ti, 16.1.

[L<sub>2</sub>Ti<sub>2</sub>( $\mu$ -O)Cl<sub>4</sub>]Cl·2H<sub>2</sub>O (10). An argon-purged mixture of TiCl<sub>3</sub> (0.50 g, 3.25 mmol) in dry dmf (25 mL) was heated to reflux for 2 h after which time L (0.80 g, 4.6 mmol) was added to the still hot solution. After heating to reflux for further 30 min water (0.50 mL) and air ( $\approx$ 1 mL) were added. Upon cooling of the resulting solution to 0 °C, a blue precipitate formed which was collected by filtration and recrystallized from dichloromethane. Yield: 0.96 g (45%). Anal. Calcd for C<sub>18</sub>H<sub>45</sub>N<sub>6</sub>O<sub>3</sub>Cl<sub>5</sub>Ti<sub>2</sub>: C, 32.4; H, 6.8; N, 12.6; Cl, 26.5; Ti, 14.3. Found: C, 32.2; H, 6.7; N, 12.5; Cl, 27.0; Ti, 14.5.

[L<sub>2</sub>Ti<sub>2</sub>( $\mu$ -O)Cl<sub>4</sub>]Cl<sub>2</sub>·2.5H<sub>2</sub>O (11). 10 (0.2 g, 0.2 mmol) was dissolved in acetonitrile (25 mL). The solution was stirred in the presence of air at 20 °C until a clear colorless solution was obtained. Removal of half of the reaction volume by rotary evaporation led to the crystallization of a colorless solid material which was collected by filtration, washed with diethyl ether, and air-dried. Yield: 0.10 g (50%). Anal. Calcd for C<sub>18</sub>H<sub>46</sub>N<sub>6</sub>O<sub>3.5</sub>Cl<sub>6</sub>Ti<sub>2</sub>: C, 30.4; H, 6.5; N, 11.8; Ti, 13.5. Found: C, 30.6; H, 6.3; N, 11.6; Ti, 13.8.

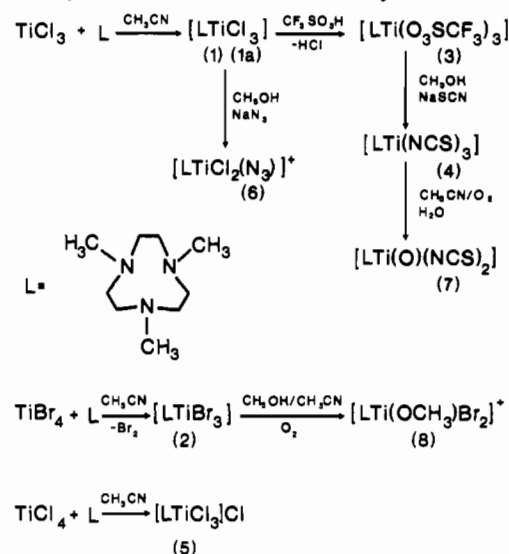
[L<sub>2</sub>Ti<sub>2</sub>( $\mu$ -O)(OH)<sub>2</sub>(O)<sub>2</sub>]·8H<sub>2</sub>O (12). 1 (0.30 g, 1.0 mmol) was dissolved in boiling water in the presence of air. After a clear colorless solution was obtained, the pH of the solution was adjusted to 7 by addition of NaHCO<sub>3</sub>. Slow cooling of the solution to 20 °C resulted in the formation of colorless crystals. Yield: 0.01 g (15%). Anal. Calcd for C<sub>18</sub>H<sub>60</sub>N<sub>6</sub>O<sub>13</sub>Ti<sub>2</sub>: C, 32.5; H, 9.1; N, 12.6. Found: C, 32.3; H, 8.9; N, 12.5.

[L<sub>2</sub>Ti<sub>2</sub>(O)<sub>2</sub>( $\mu$ -F)](PF<sub>6</sub>) (13). A solution of 1 (0.30 g, 1.0 mmol) and NaF (0.10 g, 2.3 mmol) in a mixture of nitromethane (25 mL) and water (5 mL) was heated to reflux for 30 min in the presence of air. To the then yellow solution sodium hexafluorophosphate (1.0 g) was added. A microcrystalline yellow solid precipitated which was recrystallized from a minimum amount of nitromethane. Yield: 0.30 g (90%). Anal. Calcd for C<sub>18</sub>H<sub>42</sub>N<sub>6</sub>O<sub>2</sub>F<sub>9</sub>PTi<sub>2</sub>: C, 32.3; H, 6.45; N, 12.4; F, 25.6; Ti, 14.2. Found: C, 31.9; H, 6.3; N, 12.5; F, 25.5; Ti, 14.4.

**Physical Measurements.** Infrared spectra were recorded in the range 4000–400 cm<sup>-1</sup> as KBr disks on a Perkin-Elmer FT-IR spectrometer Model 1720 X; in the range 400–200 cm<sup>-1</sup> a Bruker IFS-85 spectrometer (CsI disks) was used. The Raman spectrum of a solid sample of 7 was recorded on a Perkin-Elmer FT-IR 1760 X model with additional Raman equipment FT-Raman 1700 X by using a Nd YAG laser (1064-nm, 0.4-W output). Electronic absorption spectra were recorded in the range 200–2000 nm on a Perkin-Elmer Lambda 9 spectrophotometer. Cyclic voltammetric measurements were carried out by the use of PAR equipment (potentiostat Model 173, universal programmer Model 175) on acetonitrile solutions that contained 0.1 M tetra-*n*-butylammonium hexafluorophosphate ([TBA]PF<sub>6</sub>) as the supporting electrolyte and  $\approx 1.0 \times 10^{-3}$  M complex. *E*<sub>1/2</sub> values, determined as (*E*<sub>p,a</sub> + *E*<sub>p,c</sub>)/2, were referenced to the Ag/AgCl electrode (LiCl, C<sub>2</sub>H<sub>5</sub>OH) at ambient temperature and are uncorrected for junction potentials. Under our experimental conditions, the ferrocenium/ferrocene couple is at *E*<sub>1/2</sub> = +0.51 V vs Ag/AgCl. Magnetic susceptibilities of powdered samples were measured by using the Faraday method in the temperature range 80–298 K. Corrections for diamagnetism were applied with use of Pascal's constants.

<sup>1</sup>H NMR spectra were recorded on a Bruker WP 80 NMR spectrometer (80.13 MHz) and a Bruker AM 400 NMR spectrometer (400.13 MHz).

## Scheme I. Syntheses of Mononuclear Complexes



The deuterated solvents were used as internal standards. The <sup>19</sup>F NMR spectrum of 13 was recorded on a Bruker WP 89 spectrometer (54.13 MHz) with internal standard CFCl<sub>3</sub>.

**X-ray Crystallography.** Crystal data, data collection, and refinement are summarized in Table I (and corresponding tables in the supplementary material). Graphite-monochromated Mo K $\alpha$  X radiation was used throughout. Unit cell parameters were determined in all cases (1, 1a, 7, 8, and 13) by the automatic indexing of 25–35 centered reflections. Intensity data were corrected for Lorentz, polarization, and absorption effects (empirical  $\psi$ -scans of seven reflections in the range  $6 \leq 2\theta \leq 50^\circ$ ) in the usual manner. For 1 and 1a numerical absorption corrections on the basis of 14 crystal faces, respectively were applied. The structures were solved by conventional Patterson and difference Fourier (1, 1a, 7) and direct methods (8, 13) by using the SHELXTL-PLUS program package.<sup>23</sup> The function minimized during full-matrix least-squares refinement was  $\sum w(|F_o| - |F_c|)^2$  where  $w = 1/\sigma^2(F)$ . Neutral-atom scattering factors and anomalous dispersion corrections for non-hydrogen atoms were taken from ref 24. The positions of the hydrogen atoms in 1 and 1a were located in the difference Fourier map and were refined with variable positional parameters and fixed isotropic thermal parameters *U*<sub>iso</sub> (1, 0.04 Å<sup>2</sup>; 1a, 0.06 Å<sup>2</sup>); those of all other structures were placed at calculated positions with group isotropic thermal parameters (methylene H atoms) while the methyl groups were treated as rigid bodies. All non-hydrogen atoms were refined with anisotropic thermal parameters. Specific details of X-ray structure determinations are given below.

**1 and 1a.** When the refined atom coordinates of 1 were used as starting set for the structure solution of 1a, an initial *R* value of only 0.20 was

(23) Sheldrick, G. M. Full-matrix least-squares structure refinement program package SHELXTL-PLUS, University of Göttingen.

(24) *International Tables of Crystallography*; Kynoch: Birmingham, England, 1974; Vol. IV, pp 99, 149.

**Table II.** Electronic Spectra<sup>a</sup> and Magnetic Properties of the Complexes

complex	$\lambda_{\text{max}}$ , nm ( $\epsilon$ , L·mol <sup>-1</sup> ·cm <sup>-1</sup> )	magnetism, <sup>b</sup> $\mu_{\text{eff}}/\mu_{\text{B}}$
1	690 (30)	1.7
1a	390, 690 (30)	1.7
2	295 (4.1 × 10 <sup>3</sup> ), 720 (27)	1.7
3	nm <sup>c</sup>	1.7
4	nm	1.6
5	380 (350)	diamagnetic
6	nm	diamagnetic
7	230 (3.4 × 10 <sup>4</sup> ), 285 (sh), 306 (1.3 × 10 <sup>4</sup> )	diamagnetic
8	284 (5.8 × 10 <sup>3</sup> ), 381 (2.0 × 10 <sup>3</sup> )	diamagnetic
9	570 (520), 750 (sh), 940 (sh)	2.35
10	570 (255), 750 (sh), 940 (sh)	1.70
11	nm	diamagnetic
12	nm	diamagnetic
13	nm	diamagnetic

<sup>a</sup> Measured in CH<sub>3</sub>CN solution at 20 °C. <sup>b</sup> Temperature-independent magnetic moments measured in the temperature range 85 to 298 K. <sup>c</sup> Not measured.

obtained. Subsequent refinement of **1a** resulted in systematic shifts of the starting coordinates,  $x, y, z$  (Table IV) to  $1/2 - x, y, z$  (supplementary material). A pseudomirror plane running through Ti ( $x = 0.244$ ), C13 ( $x = 0.252$ ), and N7 ( $x = 0.246$ ) is generated within one molecule of  $\text{LTiCl}_3$ .

(7). It has not been possible to discern unambiguously between the centric and acentric space group from  $E$ -value statistics. We have fully refined the structure in both space groups. We have decided that refinement in the acentric space group is probably correct since the goodness-of-fit index is 2.63 whereas in the centric space group this index is 4.35. The question really depends on the location of C1 and C2 relative to each other only. In the centric space group the C1–C2 bond is bisected by a crystallographic mirror plane which imposes crystallographic site symmetry  $m$  on the  $\text{LTi}(\text{O})(\text{NCS})_2$  molecule. This is not compatible with  $(\lambda\lambda\lambda)$  or  $(\delta\delta\delta)$  conformation of the five-membered chelate rings

$\text{Ti-N-C-C-N}$ , and a disorder of both forms would prevail. On the other hand, refinement in the acentric space group also gave an unrealistically short C1–C2 bond length, indicating also some degree of disorder. Therefore, it has not been possible to determine the absolute configuration of  $[\text{LTi}(\text{O})(\text{NCS})_2]$  molecules in the crystal investigated.

(8). The structure refined smoothly in the centric space group only. The perchlorate anions and the methylene groups of the coordinated macrocycle L show some degree of disorder.

(13). It has not been possible to discern crystallographically between terminal oxo and fluoride ligands (O1 and F2) in the dinuclear cation of **13**. This problem is often encountered in the crystallography of oxo/tetrafluorotitanium(IV) complexes.

## Results

**Syntheses and Spectroscopic Characterization of Mononuclear Complexes.** Scheme I summarizes the synthetic routes to new mononuclear titanium(III) and -(IV) complexes. Table II summarizes their electronic spectra and magnetic properties. Due to its relative insensitivity toward oxygen and moisture *fac*-tris(acetonitrile)trichlorotitanium(III) is frequently used as starting material for the synthesis of titanium(III) complexes rather than its also available analogues  $\text{TiA}_3\text{X}_3$  ( $A = \text{tetrahydrofuran, dioxane, pyridine; X} = \text{Cl, Br, I}$ ).<sup>25</sup> Reaction of  $(\text{CH}_3\text{CN})_3\text{TiCl}_3$  in acetonitrile with the macrocycle 1,4,7-trimethyl-1,4,7-triazacyclononane (L) under an argon atmosphere at 20 °C affords blue crystals of  $[\text{LTiCl}_3]$  in 92% yield. To our surprise we obtained blue-green or even light-green crystalline precipitates (**1a**) when the same reaction was carried out at elevated temperature (reflux) by using otherwise identical reaction conditions. Both materials

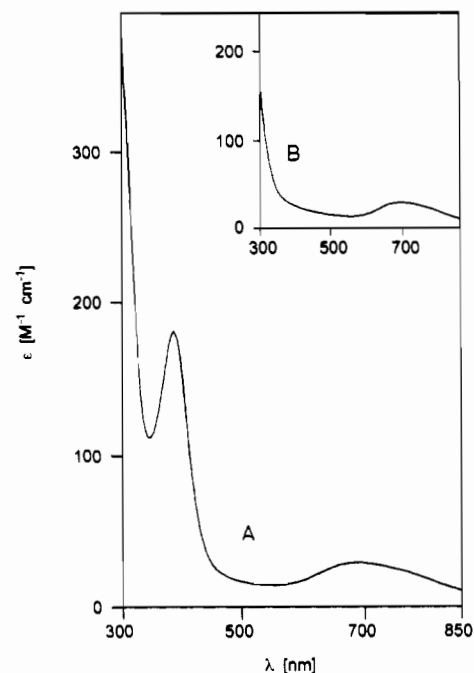


**Figure 1.** Electronic spectra of acetonitrile solutions of green **1a** (spectrum A) and blue **1** (inset B) at 20 °C.

**1** and **1a** analyzed as  $[\text{LTiCl}_3]$  although—with hindsight—we found that for **1a** the chloride content appeared to be consistently slightly lower than is required for the formulation as  $[\text{LTiCl}_3]$ . Green precipitates of **1a** were also obtained from acetonitrile solutions of  $\text{TiCl}_4$  which were heated to reflux and to which L was added. Refluxing blue **1** in acetonitrile produced green **1a**.

From temperature-dependent susceptibility measurements using a Faraday balance in the range 80–298 K on powdered samples of **1** and **1a**, we calculated a temperature-independent magnetic moment of 1.7  $\mu_{\text{B}}/\text{Ti}$  for both **1** and **1a** as expected for the spin-only value of an octahedral titanium(III) complex ( $d^1$ ).

As we will describe in detail below, single-crystal X-ray structure determinations of **1** and **1a** revealed that both materials seem to consist exclusively of neutral  $[\text{LTiCl}_3]$  molecules.

The first indication that **1a** contains an unknown impurity was obtained from the electronic absorption spectra of **1** and **1a** dissolved in acetonitrile. The inset in Figure 1 shows the spectrum of a blue solution of **1** which shows one absorption maximum in the visible region at 690 nm ( $\epsilon = 30 \text{ L}\cdot\text{mol}^{-1}\cdot\text{cm}^{-1}$ ). The spectrum of a green solution of **1a** shows this absorption maximum in the visible region at the same wavelength which, within experimental error of weighting of samples, has the same molar absorption coefficient as **1** but in contrast to **1** a second absorption maximum is observed for **1a** at 390 nm. A key observation is that the ratio of the apparent molar absorption coefficients of the absorptions at 690 and 390 nm is not constant for different preparations of **1a** whereas for **1** always the same spectrum is observed. This indicates that the two maxima of **1a** cannot belong to the same species. A further remarkable feature is that anaerobic green solutions of **1a** change color within 20 min to blue upon addition of a few drops of water. Figure 2 shows a scan spectrum of this reaction. The band at 390 nm disappears whereas the intensity of the band at 690 nm decreases only marginally with time. The original spectrum of **1a** can be regenerated immediately by passing a stream of gaseous HCl through the above solution.

What is the nature of the species which displays the absorption at 390 nm? It should be a yellow compound if no further bands in the visible region are present. A mixture of this presumed yellow impurity and the blue  $[\text{LTiCl}_3]$  complex would result in a green solution (or crystal if the two species cocrystallize).

Figure 3 shows the infrared spectra of blue crystals of **1** and a bluish-green sample of **1a** (KBr disk, 300 mg, and 1.2 mg of **1** and **1a**, respectively) in the 1500–450- $\text{cm}^{-1}$  range. Not surprisingly, many bands due to vibrations of the coordinated

(25) (a) Fowles, G. W. A.; Hoodless, R. A. *J. Chem. Soc.* **1963**, 33. (b) Schmuldbach, C. D.; Hinkley, C. C.; Kolich, C.; Ballantine, T. A. *Inorg. Chem.* **1974**, *13*, 2026. (c) Fowles, G. W. A.; Lester, T. E.; Russ, B. *J. J. Chem. Soc. A* **1968**, 805. (d) McDonald, G.; Thomson, M.; Larsen, E. M. *Inorg. Chem.* **1968**, *4*, 648. (e) Rosset, J.-M.; Floriani, C.; Mazzanti, M.; Villa, C.; Guastini, C. *Inorg. Chem.* **1990**, *29*, 3991. (f) Hoff, G. R.; Brubaker, C. H., Jr. *Inorg. Chem.* **1971**, *10*, 2063.

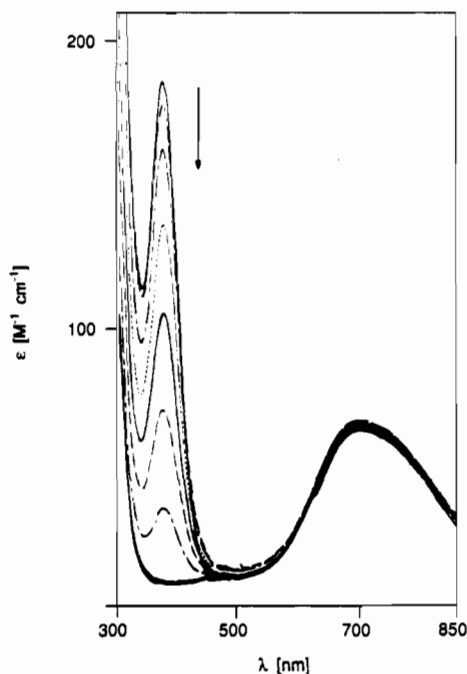


Figure 2. Scan spectrum of an acetonitrile solution of green **1a** under an argon atmosphere to which a few drops of water have been added (spectra were recorded at 2-min intervals).

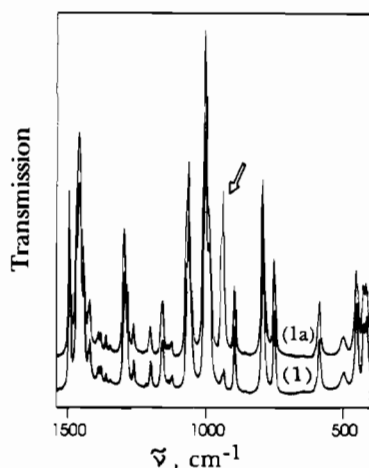
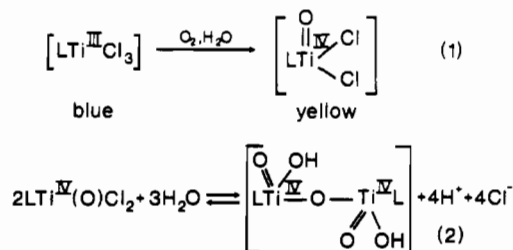


Figure 3. Infrared spectra of (a, bottom) blue crystals of **1** and (b, top) green crystals of **1a** in the 1500–500-cm<sup>-1</sup> range (300 mg of KBr; 1.2 mg of **1** and **1a**, respectively). The spectra are offset for the sake of clarity. The arrow marks the band at 938 cm<sup>-1</sup>.

macrocycle are observed. The two spectra are nearly identical with respect to both the number and position of bands and even their respective intensities. One remarkable exception is evident: Both species display a band at 938 cm<sup>-1</sup>, which is very weak in pure blue **1** but of medium intensity in green **1a**. For different preparations of **1a** it is this band which appears with increasing intensity the lighter green the crystals are.

We suggest that **1a** contains a yellow impurity with a Ti=O group which exhibits a  $\nu(\text{Ti}-\text{O})$  stretching frequency at 938 cm<sup>-1</sup>. The fact that this species cocrystallizes with blue [LTiCl<sub>3</sub>] implies that its overall structural features should be very similar to those of the main component [LTiCl<sub>3</sub>]. The monomeric neutral titanium(IV) complex [LTi(O)Cl<sub>2</sub>] would meet these requirements. It could be envisaged that this complex is formed from [LTiCl<sub>3</sub>] by reaction with a small amount of water in the solvent acetonitrile and by adventitiously present oxygen, eq 1. [LTi(O)Cl<sub>2</sub>] could in the presence of more water form [L<sub>2</sub>Ti<sub>2</sub>O<sub>2</sub>(OH)<sub>2</sub>( $\mu$ -O)]—a colorless species which we have been able to synthesize and fully characterize (see below). Concentrated HCl, on the other hand, could break the Ti—O—Ti group with regeneration of [LTi(O)Cl<sub>2</sub>]. This chemistry could explain the



reversible green to blue color change of acetonitrile solutions of **1a** upon addition of H<sub>2</sub>O or HCl, eq 2.

Despite many attempts to prepare a pure sample of [LTi(O)Cl<sub>2</sub>] we have not been able to obtain this species. Much of the synthetic chemistry described below has been undertaken to do this. In particular, we were interested in preparing and structurally characterizing a genuine octahedral titanyl complex.

Reaction of TiBr<sub>4</sub> and TiCl<sub>4</sub> at room temperature with L in dry acetonitrile afforded a green precipitate of [LTi<sup>III</sup>Br<sub>3</sub>] (**2**) and pale yellow microcrystalline solid [LTi<sup>IV</sup>Cl<sub>3</sub>]Cl (**5**), respectively. With TiBr<sub>4</sub> a redox reaction occurs whereas with TiCl<sub>4</sub> a simple substitution reaction takes place. As noted above, if TiCl<sub>4</sub> in CH<sub>3</sub>CN is heated to reflux, a green solution is obtained. Addition of L initiates then the precipitation of green "[LTiCl<sub>3</sub>]<sup>+</sup>". Redox reactions of titanium(IV) halides with simple tertiary amines are known.<sup>25a,26</sup>

The infrared spectrum of **2** in the range 400–4000 cm<sup>-1</sup> is virtually identical with that of **1**. In particular, only a very weak band at 938 cm<sup>-1</sup> is observed (as in pure samples of **1**). Thus **2** is not contaminated by a titanyl species. In agreement with this notion is the electronic spectrum of **2** measured in acetonitrile which exhibits one absorption maximum at 720 nm ( $\epsilon = 27 \text{ L}\cdot\text{mol}^{-1}\cdot\text{cm}^{-1}$ ) and a charge-transfer (CT) band at 295 nm ( $4.1 \times 10^3 \text{ L}\cdot\text{mol}^{-1}\cdot\text{cm}^{-1}$ ); no absorption at 390 nm has been detected.

The infrared spectrum of **5** also lacks a band at ca. 940 cm<sup>-1</sup>, which could be assigned to a Ti=O group,<sup>27</sup> but its electronic spectrum in acetonitrile solution shows a CT band at 380 nm ( $\epsilon = 350 \text{ L}\cdot\text{mol}^{-1}\cdot\text{cm}^{-1}$ ), which is responsible for the yellow color of **5**. The salt **5** does not cocrystallize with [LTiCl<sub>3</sub>]; it cannot be the impurity in **1a**.

[LTiCl<sub>3</sub>] (**1**) proved to be fairly substitution inert. Therefore, we attempted to replace the chloro ligands by a better leaving group such as trifluoromethanesulfonate. Reaction of **1** and CF<sub>3</sub>SO<sub>3</sub>H under an argon atmosphere at -5 °C produced a deep blue solution and gaseous HCl. Upon addition of dry diethyl ether blue [LTi(O<sub>3</sub>SCF<sub>3</sub>)<sub>3</sub>] (**3**) precipitated. **3** is very oxygen- and moisture-sensitive. The temperature-independent (80–293 K) magnetic moment of 1.7  $\mu_B$  is indicative of titanium(III).

Complex **3** reacts with NaSCN in methanol readily with immediate precipitation of [LTi<sup>III</sup>(NCS)<sub>3</sub>] (**4**). Bands at 2050 and 2020 cm<sup>-1</sup> in the infrared spectrum indicate N-bound NCS-ligands. A magnetic moment of 1.6  $\mu_B$  is again in agreement with the presence of titanium(III).

Compound **4** is quite sensitive to oxidation. The purple color of an acetonitrile solution of **4** disappeared within minutes at 55 °C. When such a yellow solution was allowed to stand in an open vessel for 48 h, a yellow microcrystalline precipitate formed which was recrystallized from an acetonitrile/water mixture (4:1). These diamagnetic orange crystals analyzed as [LTi<sup>IV</sup>(O)(NCS)<sub>2</sub>] (**7**). The X-ray structure determination (see below) confirms the monomeric octahedral structure of **7** with a terminal oxo ligand. In the infrared spectrum strong bands at 2039 and 943 cm<sup>-1</sup> (Figure 4a) are indicative of N-coordinated thiocyanate and a Ti=O group, respectively. Figure 4b shows the Raman spectrum of **7**. The strongest bands at 2049, 2038, and 2015 cm<sup>-1</sup> are assigned to  $\nu(\text{NCS})$  stretching modes. The very strong band at

(26) Antler, M.; Laubengayer, A. W. *J. Am. Chem. Soc.* **1955**, *77*, 5250.

(27) The infrared spectrum of **5** in the region 400–200 cm<sup>-1</sup> shows two (TiCl) stretching modes at 370 and 350 cm<sup>-1</sup> (A<sub>1</sub> and E in C<sub>3v</sub> symmetry).

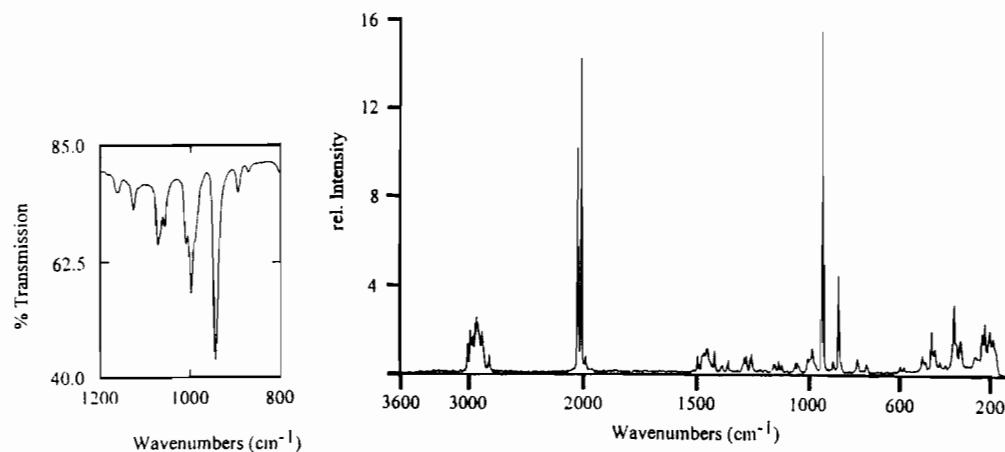


**Figure 4.** (a, Left) infrared spectrum of **7** in the range 800–1200  $\text{cm}^{-1}$  (KBr disk). (b, right) FT-Raman spectrum of solid **7** recorded with a Nd laser (1064 nm).

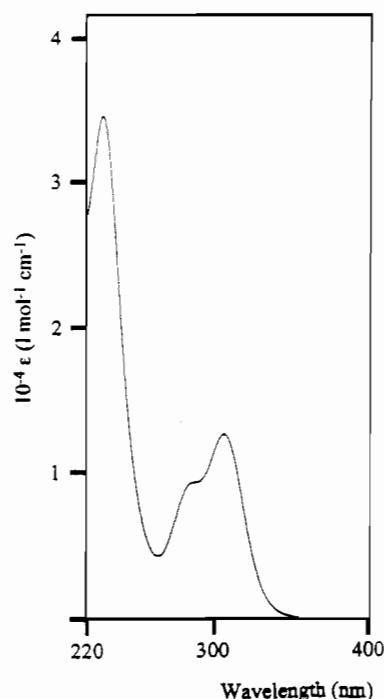


**Figure 5.** Electronic spectrum of an acetonitrile solution of **7**.

942  $\text{cm}^{-1}$  is the  $\nu(\text{Ti}=\text{O})$  stretching frequency. All other weak bands in the region 600–3600  $\text{cm}^{-1}$  are due to vibrational modes of the coordinated amine. Figure 5 shows the electronic spectrum of an acetonitrile solution of **7**. Three CT absorption maxima are observed at 320 ( $\epsilon = 3.4 \times 10^4 \text{ L}\cdot\text{mol}^{-1}\cdot\text{cm}^{-1}$ ), 285 (sh,  $9.3 \times 10^3 \text{ L}\cdot\text{mol}^{-1}\cdot\text{cm}^{-1}$ ), and 306 nm ( $12.6 \times 10^3 \text{ L}\cdot\text{mol}^{-1}\cdot\text{cm}^{-1}$ ).  $\text{NCS}^-$  is a much weaker  $\pi$ -donor as compared to chloride. Thus the electronic spectrum of the presumed  $[\text{LTi}(\text{O})\text{Cl}_2]$  species could exhibit this CT band at 390 nm. We do not assign this transition as a pure oxygen-to-titanium(IV) CT band because  $[\text{L}_2\text{Ti}_2(\text{O})_2(\text{OH})_2(\mu\text{-O})\cdot 8\text{H}_2\text{O}]$ , which also contains a terminal oxo ligand, is colorless and does not exhibit absorption maxima  $>300$  nm.

It is noteworthy in this respect that **1** reacts in methanol with excess azide with formation of dinitrogen, titanium(IV), and an unidentified amine ( $\text{NH}_3$ ). Addition of  $\text{Na}[\text{BPh}_4]$  to such a colorless reaction mixture initiated the precipitation of colorless  $[\text{LTiCl}_2(\text{N}_3)][\text{BPh}_4]$  (**6**). In the infrared spectrum of **6** a  $\text{N}_3$  stretching frequency is observed at 2085  $\text{cm}^{-1}$ . An  $\text{N}_4\text{Cl}_2^-$  donor set coordinated to a Ti(IV) ion does not give rise to a CT band in the electronic spectrum at  $\approx 390$  nm.

Air oxidation of **2** in methanol gives a yellow solution from which, upon addition of  $\text{NaClO}_4$ , yellow crystals of  $[\text{LTi}(\text{O}(\text{CH}_3)\text{Br}_2)(\text{ClO}_4)]$  (**8**) precipitated. The X-ray crystal structure de-

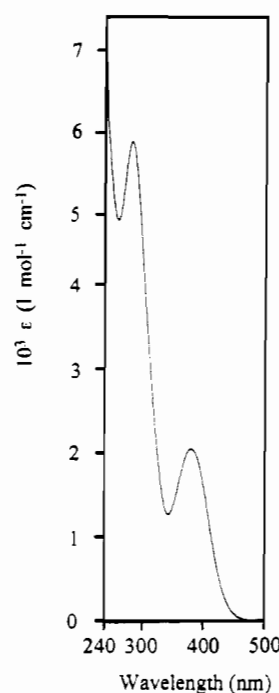


**Figure 6.** Electronic spectrum of an acetonitrile solution of **8**.

termination (see below) shows that an octahedral titanium(IV) complex with an  $\text{N}_3\text{OBr}_2$  donor set is formed, which contains a coordinated methoxy, two bromide, and a tridentate amine ligand. Figure 6 shows the electronic spectrum of **8** dissolved in acetonitrile. Clearly, two CT bands at 284 nm ( $\epsilon = 5.8 \times 10^3 \text{ L}\cdot\text{mol}^{-1}\cdot\text{cm}^{-1}$ ) and, most interestingly, at 381 ( $2.0 \times 10^3 \text{ L}\cdot\text{mol}^{-1}\cdot\text{cm}^{-1}$ ) are observed. **8** resembles structurally and electronically most closely the presumed  $[\text{LTi}(\text{O})\text{Cl}_2]$  impurity in **1a**.

If one assumes that the molar absorption coefficient of the 390-nm absorption of the presumed  $[\text{LTi}(\text{O})\text{Cl}_2]$  impurity in **1a** is of the same order of magnitude as the 381-nm absorption of **8**, one can estimate that the sample of **1a** used for the recording of the infrared spectrum (Figure 3) and for the X-ray structure determination contains  $\approx 10\%$  of this species.

**Syntheses and Characterization of Dinuclear Complexes.** Since our attempts to generate a pure sample of  $\text{LTi}(\text{O})\text{Cl}_2$  have failed so far, we decided to take a closer look at the behavior of  $[\text{LTiCl}_3]$  (**1**) under hydrolytic and oxidative reaction conditions. As we will show, this leads to dinuclear complexes with linear Ti–O–Ti structural units. Some aspects of this work have been communicated previously.<sup>13</sup> Scheme II summarizes the synthetic routes employed.

When a crystalline sample of **1** was dissolved in deoxygenated dimethylformamide (dmf) which contained  $\approx 2\%$  of water or,



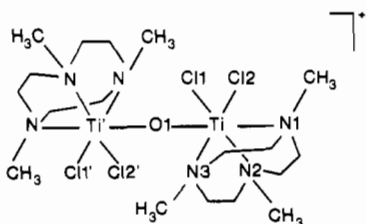
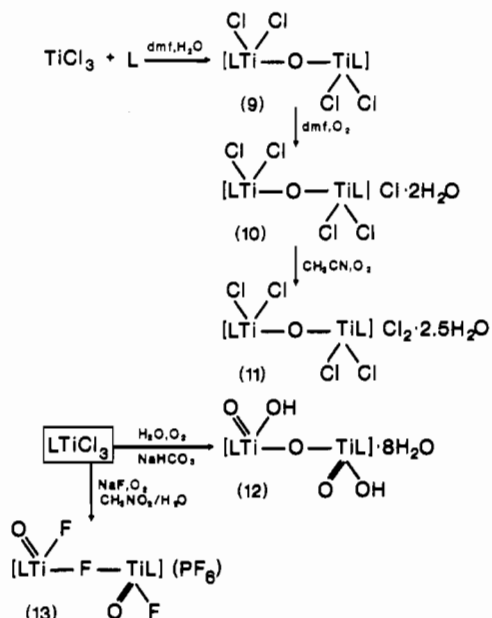


**Figure 7.** Structure of the mixed-valence dinuclear cation in **10**.<sup>13</sup> Important bond lengths: Ti–O1 1.872 (1), Ti–Cl1 2.319 (2), Ti–Cl2 2.321 (2), Ti–N1 2.340 (5), Ti–N2 2.241 (5), Ti–N3 2.237 (4) Å. Bond angle: Ti–O1–Ti 180.0°.

### Scheme II. Syntheses of Dinuclear Complexes



alternatively, when  $\text{TiCl}_3$  and the macrocycle **L** were dissolved in the same solvent under strictly anaerobic conditions, a clear, deep blue solution was obtained after heating the mixtures to reflux for 30 min. Upon cooling to ambient temperature, a blue precipitate formed in 24% yield, which was washed several times with  $\text{CH}_2\text{Cl}_2$ . The blue residue analyzed as  $[\text{L}_2\text{Ti}_2\text{Cl}_4(\mu\text{-O})]$  (**9**).

In the infrared spectrum of **9** a strong band at  $745\text{ cm}^{-1}$  is assigned to the  $\nu(\text{Ti}\text{--}\text{O}\text{--}\text{Ti})$  stretching mode. This band is absent in the spectrum of **1**. The electronic spectrum of **9** in  $\text{CH}_3\text{CN}$  displays an asymmetric absorption maximum at  $570\text{ nm}$  ( $\epsilon = 520\text{ L}\cdot\text{mol}^{-1}\cdot\text{cm}^{-1}$ ) with shoulders at  $750$  and  $940\text{ nm}$ . Interestingly, no absorption at  $380\text{ nm}$  is detected where in fact an absorption minimum is observed. From temperature-dependent susceptibility measurements ( $80\text{--}295\text{ K}$ ) a temperature-independent magnetic moment of  $1.66\ \mu_{\text{B}}/\text{Ti}$  is calculated. Since this value corresponds closely to the spin-only value of a  $\text{Ti}(\text{III})$  ion, we conclude that the spins of the two unpaired electrons in **9** are uncoupled. An explanation for this behavior has been given in ref 28.

When the same reaction as described above was carried out in the presence of a small amount of air ( $1\text{--}2\text{ mL}$  were added by using a syringe), again a blue precipitate was obtained in 45% yield which is soluble in  $\text{CH}_2\text{Cl}_2$  or  $\text{CHCl}_3$  in contrast to **9**. The elemental analysis of a sample which was recrystallized from  $\text{CH}_2\text{Cl}_2$  showed a ratio  $\text{Ti}:\text{L}:\text{Cl}$  of  $1:1:2.5$ . The X-ray structure determination (Figure 7) showed that the mixed-valent compound  $[\text{L}_2\text{Ti}_2\text{Cl}_4(\mu\text{-O})]\text{Cl}\cdot 2\text{H}_2\text{O}$  (**10**) had formed.<sup>13</sup> A magnetic moment of  $1.7\ \mu_{\text{B}}/\text{dinuclear unit}$  ( $80\text{--}298\text{ K}$ ) indicates the presence of one unpaired electron per dinuclear unit. The  $\text{Ti}\text{--}\text{O}\text{--}\text{Ti}$  stretching mode is observed at  $745\text{ cm}^{-1}$ . The electronic spectrum of **11** is very similar to that of **9** except that the intensity of the absorption at  $570$ ,  $750$  (sh), and  $940$  (sh) is only half of **9**. Although

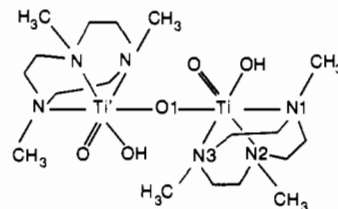


**Figure 8.** Atom connectivity of the neutral dinuclear molecule in crystals of **12**, as determined by X-ray crystallography. Preliminary bond lengths: Ti–O<sub>bridge</sub> 1.84 (1), Ti–O<sub>terminal</sub> 1.76 (1), Ti–O<sub>hydroxo</sub> 1.83 (1) Å.

the complex cation lies on a crystallographic center of symmetry (i.e. both the titanium(III) and -(IV) ions are crystallographically equivalent), we have not found spectroscopic evidence for delocalization of the valences. Therefore, we argue that **10** is a class I species according to Robin and Day<sup>29</sup> with localized oxidation states. Complex **10** can be electrochemically reversibly reduced and oxidized by one electron (see below). This is also chemically possible. Thus a solution of **10** in acetonitrile exposed to air changes color rapidly from blue to colorless. From such a solution colorless crystals of  $[\text{L}_2\text{Ti}^{\text{IV}}_2\text{Cl}_4(\mu\text{-O})]\text{Cl}_2\cdot 2.5\text{H}_2\text{O}$  (**11**) were obtained. The  $\text{Ti}\text{--}\text{O}\text{--}\text{Ti}$  stretching frequency of **11** is observed at  $745\text{ cm}^{-1}$ . The  $80\text{-MHz } ^1\text{H NMR}$  spectrum of **11** in  $\text{CD}_3\text{NO}_2$  clearly shows two singlets at  $\delta = 2.35$  (6 H) and  $4.7$  (12 H) in the ratio  $1:2$ , which are assigned to methyl protons and a multiplet at  $\delta 2.8\text{--}4.1$  corresponding to 24 methylene protons of two macrocyclic ligands in agreement with the structure depicted in Figure 7.

A solution of **1** in water at  $100\text{ }^\circ\text{C}$  produced in the presence of air a colorless solution. When the pH of this acidic solution was adjusted to 7 by adding solid  $\text{NaHCO}_3$ , colorless, chloride-free crystals of  $[\text{L}_2\text{Ti}(\text{O})_2(\text{OH})_2(\mu\text{-O})]8\cdot\text{H}_2\text{O}$  (**12**) slowly precipitated. Thus complete hydrolysis of all  $\text{Ti}\text{--}\text{Cl}$  bonds and oxidation occur under these experimental conditions. The translucent crystals of **12** became turbid within 48 h of standing in a normal laboratory atmosphere. This process is accompanied by loss of water molecules of crystallization. The results of an X-ray structure determination<sup>30</sup> confirm the dinuclear nature of **12**. Figure 8 shows the atom connectivity and gives some preliminary bond distances. Compound **12** contains two octahedrally coordinated  $\text{Ti}(\text{IV})$  ions which are connected by a linear oxo bridge. In addition, each  $\text{Ti}(\text{IV})$  ion is bound to a terminal oxo and hydroxo group and one macrocyclic amine **L**. A similar structure has been reported recently<sup>31</sup> for the divanadium(V) complex  $[\text{L}_2\text{V}^{\text{V}}(\text{O})_2(\text{OH})_2(\mu\text{-O})](\text{ClO}_4)_2$ . The terminal hydroxo groups were shown to be reversibly deprotonated in alkaline aqueous solution, generating  $[\text{L}_2\text{V}_2(\text{O})_4(\mu\text{-O})]$ . Attempts to isolate a similar *cis*-dioxodititanium(IV) complex  $[\text{L}_2\text{Ti}_2(\text{O})_4(\mu\text{-O})]^{2-}$  failed. When **12** was dissolved in water and the pH was increased to  $>7$  slow decomposition of  $\text{TiO}_2(\text{aq})$  was observed. The electronic spectrum of **12** is featureless  $>300\text{ nm}$ .

Finally, we found that the reaction of **1** and  $\text{NaF}$  dissolved in nitromethane, which contained ca. 5% of water, produced in the presence of air a yellow clear solution. Upon addition of  $\text{NaPF}_6$  yellow crystals of  $[\text{L}_2\text{Ti}_2(\text{O})_2\text{F}_2(\mu\text{-F})](\text{PF}_6)$  (**13**) precipitated. The X-ray structure determination (see below) clearly shows the corner-sharing bioctahedral nature of the species but it has not been possible to distinguish crystallographically between terminal fluoride and oxide ligands. Therefore, a number of geometrical isomers are in principle possible (Figure 10).

The terminal  $\text{Ti}=\text{O}$  groups were unambiguously identified in the infrared spectrum of **13** which displays a strong  $\nu(\text{Ti}=\text{O})$  stretching mode at  $938\text{ cm}^{-1}$ . Only one other band not due to the  $\text{PF}_6$  anion or the coordinated macrocycle **L** has been observed at  $617\text{ cm}^{-1}$ , which could be assigned either to the  $\nu(\text{Ti}\text{--}\text{F})$  stretching

(28) Bodner, A.; Drücke, S.; Wieghardt, K.; Nuber, B.; Weiss, J. *Angew. Chem., Int. Ed. Engl.* **1990**, *29*, 68.

(29) Robin, M. B.; Day, P. *Adv. Inorg. Chem. Radiochem.* **1967**, *8*, 357.

(30) Details of this X-ray structure determination will be reported elsewhere.

(31) Knopp, P.; Wieghardt, K.; Nuber, B.; Weiss, J.; Sheldrick, W. S. *Inorg. Chem.* **1990**, *29*, 363.

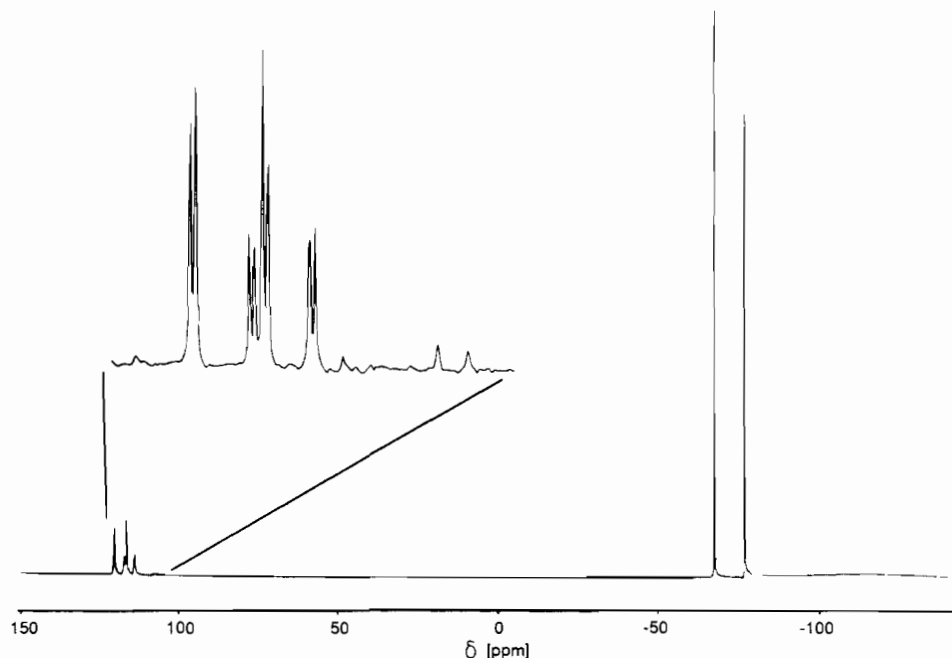


**Figure 9.**  $^{19}\text{F}$  NMR spectrum ( $\text{CH}_3\text{NO}_2$ ,  $\text{CFCl}_3$  standard; 53.39 MHz, 20 °C) of **13**. The offset displays the region  $\delta = 100\text{--}130$  ppm.

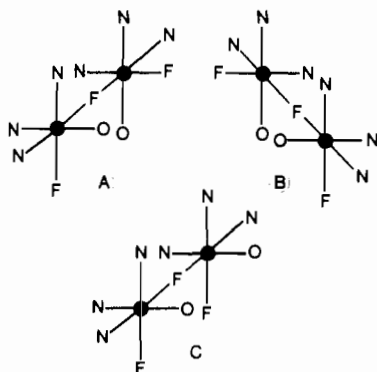


**Figure 10.** Possible isomers of **13**. A and B represent enantiomers, C the diastereomer. Complications due to  $\text{Ti-N-C-C-N}$  chelate ring conformations are not considered here.

mode of terminally bound fluoride or, alternatively, to the  $\nu(\text{Ti-F-Ti})$  stretching mode. It could in principle, also be due to a  $\nu(\text{Ti-O-Ti})$  vibration.

It is therefore important to establish unambiguously the absence of a  $\mu$ -oxo bridge and/or the presence of a bridging fluoride.  $^{17}\text{O}$  and  $^{19}\text{F}$  NMR spectroscopy are ideally suited to do this. The  $^{17}\text{O}$  NMR spectrum of **13** in  $\text{CH}_3\text{NO}_2$  exhibits only two resonances at  $\delta$  610, which is assigned to solvent oxygen, and at  $\delta$  -16.5, which is assigned to oxygen of the  $\text{Ti=O}$  group. This assignment is bolstered by the fact that for  $[\text{L}_2\text{V}_2\text{O}_4(\mu\text{-O})]$ , which contains both terminal and bridging oxygen atoms, two  $^{17}\text{O}$  NMR resonances at  $\delta$  527.6 ( $\text{V-O-V}$ ) and -11.5 ( $\text{V=O}$ ) are observed. Thus **13** does not display resonances due to bridging oxide.

Figure 9 shows the 53.39-MHz  $^{19}\text{F}$  NMR spectrum of crystals of **13** dissolved in  $\text{CH}_3\text{NO}_2$  ( $\text{CFCl}_3$  standard at 20 °C). The resonances of the  $\text{PF}_6^-$  anion, a doublet at  $\delta$  -67 and -76, are observed. Only four further resonances at  $\delta$  +115.9, 116.2, 119.8, and 120.1 in the ratio 2:1:2:1 are detectable. The inset in Figure 9 shows that each of these resonances is split by a doublet. We now consider the isomers depicted in Figure 10. The first two structures A and B are enantiomers whereas structure C is a diastereomer if we consider only the first coordination spheres of the dinuclear cation. These are formed statistically in the ratio 2:1, and they may cocrystallize because their overall geometry is very similar due to the fact that  $\text{O}^{2-}$  and  $\text{F}^-$  are isoelectronic and have very similar steric requirements. Thus the  $^{19}\text{F}$  NMR

spectrum (Figure 9) is the spectrum of a mixture of an enantiomer and a diastereomer. Each of these is represented by two doublets (ratio 2:1). Coupling between the terminal ( $\text{F}_t$ ) and the bridging fluoride ( $\text{F}_b$ ) gives a doublet; the coupling constant  $^2J_{\text{F}_t\text{F}_b}$  is 26 Hz for the more intensive resonances whereas  $^2J_{\text{F}_t\text{F}_b}$  is 23 Hz for the weaker signals. For comparison, in the corner-sharing dinuclear species  $[\text{Ti}_2\text{F}_{11}]^{3-}$   $^2J_{\text{F}_t\text{F}_b}$  is 44 Hz.<sup>32</sup> For the corresponding coupling between the bridging and the two terminal fluorides, two triplets with identical coupling constants are expected which is not observed. These triplets are only observed if the two terminal fluorides in **13** are chemically and magnetically equivalent. If this is not the case, only a doublet of doublets is expected, as is observed. Both terminal fluorides couple to a doublet with the bridging  $\text{F}_b$  but with a slightly differing chemical shift of  $(\delta(\text{F}_{t1}) - \delta(\text{F}_{t2})) = 0.3$  ppm. The coupling of  $\text{F}_b$  with  $\text{F}_t$  results also in a doublet of doublets, but the chemical shift is accidentally the same. Therefore, only one doublet of doublets for the enantiomers and the diastereomer is observed, respectively.

The assumption that the terminal fluorides in **13** are chemically not equivalent may be a consequence of the fact that the three five-membered chelate rings of each coordinated macrocycle have either  $(\lambda\lambda\lambda)$  or  $(\delta\delta\delta)$  conformation. In crystals of **13** the bridging fluoride is located on a crystallographic center of symmetry (Figure 14) and consequently in each dinuclear cation one coordinated macrocycle has  $(\lambda\lambda\lambda)$  and the other must have  $(\delta\delta\delta)$  conformation unless other static disordered forms are also present. This situation leads to different intramolecular, through-space interactions of the methyl protons of one macrocycle coordinated to  $\text{Ti1}$  with the terminal fluoride coordinated to the second  $\text{Ti1}'$  atom and vice versa only if the chelate ring conformations of both  $\text{Ti}$  centers are  $(\lambda\lambda\lambda)$  (or  $(\delta\delta\delta)$ ). In the centrosymmetric form of **13** where one macrocycle has  $(\lambda\lambda\lambda)$  and the other has  $(\delta\delta\delta)$  configuration the two through-space interactions between the methyl group and  $\text{F}_t$  would be the same. In other words, only in the noncentrosymmetric form of **13** are the two  $\text{F}_t$  not equivalent. This explanation appears to be somewhat forced. It is probably more plausible that the expected triplets appear as doublets of doublets due to concentration effects, as has been observed for  $[\text{Ti}_2\text{F}_{11}]^{3-}$ .<sup>32e</sup> In any case, the observed  $^{19}\text{F}$  NMR spectrum agrees

(32) (a) Dean, P. A. *Can. J. Chem.* 1973, 51, 4024. (b) Dean, P. A.; Evans, D. F. *J. Chem. Soc. A* 1967, 698. (c) Lee, H. G.; Dyer, D. S.; Ragsdale, R. O. *J. Chem. Soc., Dalton Trans.* 1976, 1325. (d) Dyer, D. S.; Ragsdale, R. O. *Inorg. Chem.* 1967, 6, 8. (e) Dean, P. A.; Ferguson, B. J. *Can. J. Chem.* 1974, 52, 667.



**Table III.** Summary of Electrochemical Data for the Complexes<sup>a</sup>

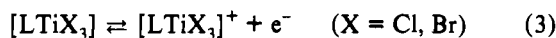
complex	scan range, V vs Ag/AgCl	redox potentials, <sup>b</sup> V vs Ag/AgCl
<b>1</b>	-1.9 to +1.9	+0.37 (r)
<b>1a</b>	same behavior as <b>1</b>	
<b>2</b>	-1.9 to +1.5	+0.53 (r)
		-1.36, -1.58 (irr)
<b>4</b>	-1.8 to +1.8	+0.50 (r)
		-1.32 (r)
<b>5</b>	same behavior as <b>1</b>	
<b>8</b>	-1.0 to +1.0	-0.06 (r)
<b>9</b>	same behavior as <b>10</b>	no irr oxidation at +1.26
<b>10</b>	-0.8 to +0.8	+0.52 (r)
		-0.38 (r)
		+1.26 (irr)
<b>11</b>	same behavior as <b>10</b>	

<sup>a</sup> Measured in dry acetonitrile at 20 °C. Conditions: 0.10 M tetra-*N*-butylammonium hexafluorophosphate, [complex] = 10<sup>-3</sup> M; Pt-button working electrode; Pt-wire auxiliary electrode; Ag/AgCl-saturated LiCl/C<sub>2</sub>H<sub>5</sub>OH reference electrode, scan rates 50–200 mV/s. <sup>b</sup>  $E_{1/2}$  (V) values ( $(E_{pa} + E_{pc})/2$ ) for reversible (r) processes and peak potentials for irreversible (irr) processes are listed.

only with a structure for **13** where one bridging and two terminal fluoride ligands are present.

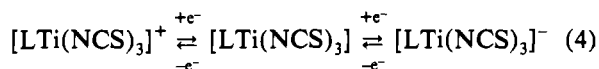
**Electrochemistry.** We have recorded the cyclic voltammograms (cvs) of a number of the new complexes in acetonitrile (0.10 M [TBA]PF<sub>6</sub> supporting electrolyte); the results are summarized in Table III.

Both **1** and **2** display one reversible one-electron-transfer process according to eq 3, as has been deduced from the diagnostic criteria and by coulometry of **1** at a fixed potential of +0.70 V vs Ag/



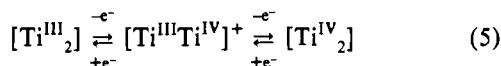
AgCl. The formal redox potential of **2** is shifted anodically as compared to **1**. Thus the +III oxidation state is stabilized in **2** compared to **1**. **5**, the oxidized form of **1**, shows the same electrochemical behavior as **1**.

Interestingly, the cv of **4** exhibits two reversible one-electron-transfer waves at  $E_{1/2} = 0.50$  V and  $E_{1/2} = -1.32$  V vs Ag/AgCl, which are assigned to the Ti(III)/Ti(IV) couple and Ti(III)/Ti(II) couple, respectively, as in eq 4. Thiocyanate in contrast



to chloride and bromide is quite a potent  $\pi$ -acceptor and may therefore stabilize the +II oxidation state. Octahedral Ti(II) complexes containing phosphane ligands as  $\pi$ -acceptor ligands have been characterized by Girolami et al.<sup>33</sup> The reduced form of **4** is stable on the time scale of a cv experiment. Attempts to isolate this species have failed.

The electrochemistry of **9–11** has been described in ref 13. They exhibit identical cvs with two reversible one-electron-transfer waves, as in eq 5.



**Description of Crystal Structures.** Table IV gives the atom coordinates of **1**; those for **1a** are available in the supplementary material. Table V summarizes important bond lengths and angles of **1** and **1a** and Figure 11 shows a perspective view of one neutral molecule in **1**. Both **1** and **1a** crystallize in the same monoclinic space group  $P2_1/c$  with very similar unit cell dimensions.

It is emphasized that both crystal structure determinations are of high quality since all protons in both structures have been located and refined (supplementary material). The resulting C–H

**Table IV.** Atom Coordinates ( $\times 10^4$ ) and Isotropic Thermal Parameters ( $\text{\AA}^2 \times 10^3$ ) blue [LTiCl<sub>3</sub>] **1**

atom	x	y	z	$U_{eq}$
Ti1	2438.7 (4)	281.8 (7)	1289.9 (3)	27.00 (8)
Cl1	3724.6 (7)	-1860.0 (1)	826.9 (8)	57.9 (3)
Cl2	895.4 (7)	-1469 (1)	975.7 (6)	43.6 (3)
Cl3	2518.3 (8)	-458 (1)	2726.2 (6)	58.1 (2)
N1	3727 (1)	2438 (3)	1434 (1)	33.6 (6)
N4	1443 (1)	2801 (3)	1480 (1)	30.6 (5)
N7	2460 (2)	1617 (3)	5 (1)	35.6 (6)
C2	3249 (2)	3792 (5)	2015 (2)	43.1 (8)
C3	2139 (2)	4385 (4)	1730 (2)	42.2 (8)
C5	901 (2)	3162 (5)	658 (2)	38.9 (7)
C6	1712 (2)	3192 (5)	-48 (2)	46.2 (9)
C8	3601 (2)	2192 (5)	-127 (2)	46.0 (9)
C9	4001 (2)	3296 (5)	603 (2)	43.7 (8)
CN1	4745 (2)	1723 (6)	1821 (3)	55.8 (12)
CN4	576 (2)	2524 (6)	2124 (2)	47.8 (9)
CN7	2158 (3)	298 (7)	-680 (2)	60.9 (13)

**Table V.** Selected Bond Lengths ( $\text{\AA}$ ) and Angles (deg) for **1** (Blue) and in Parentheses for **1a** (Green)

Ti–Cl1	2.355 (1)	(2.356 (1))
Ti–Cl2	2.353 (1)	(2.345 (1))
Ti–Cl3	2.349 (1)	(2.353 (1))
Ti–N1	2.257 (2)	(2.263 (2))
Ti–N2	2.243 (3)	(2.274 (3))
Ti–N3	2.267 (3)	(2.280 (3))
Cl1–Ti–Cl2	96.6 (1)	(97.4 (1))
Cl1–Ti–Cl3	97.0 (1)	(96.7 (1))
Cl2–Ti–Cl3	96.5 (1)	(96.9 (1))
N1–Ti–Cl1	91.4 (1)	(91.6 (1))
N1–Ti–Cl2	167.5 (1)	(164.4 (1))
N1–Ti–Cl3	92.0 (1)	(94.6 (1))
N4–Ti–Cl1	164.6 (1)	(167.3 (1))
N4–Ti–Cl2	92.0 (1)	(90.8 (1))
N4–Ti–Cl3	94.7 (1)	(91.7 (1))
N1–Ti–N4	78.1 (1)	(78.3 (1))
N7–Ti–Cl1	89.9 (1)	(93.0 (1))
N7–Ti–Cl2	93.2 (1)	(90.2 (1))
N7–Ti–Cl3	167.4 (1)	(167.1 (1))
N1–Ti–N7	77.2 (1)	(76.7 (1))
N4–Ti–N7	76.8 (1)	(77.4 (1))

distances are in the usual range 0.9–1.1  $\text{\AA}$ . The LTiCl<sub>3</sub> molecules do not possess crystallographically imposed symmetry. Since the space group  $P2_1/c$  contains a mirror plane both enantiomers

with ( $\lambda\lambda\lambda$ ) and ( $\delta\delta\delta$ ) configured  $\overline{\text{Ti–N–C–C–N}}$  chelate rings are present (the racemate crystallizes). As a consequence and in contrast to many crystal structure determinations of complexes containing an LM fragment, the coordinated macrocycles are not disordered. All C–C distances are in the range  $1.51 \pm 0.015$   $\text{\AA}$ , and the C–N distances are in the range  $1.49 \pm 0.015$   $\text{\AA}$ , which is typical for C–C and C–N single bonds. The final difference Fourier maps of **1** and **1a** show residual electron density of only 0.71 and 0.56 e $\cdot\text{\AA}^{-3}$ , respectively. Thus no indication of uncoordinated chloride ions is detectable in **1a** where [LTiCl<sub>3</sub>]Cl might have been considered an impurity. Before we discuss the details of the TiN<sub>3</sub>Cl<sub>3</sub> coordination sphere in both structures, we consider the packing of the LTiCl<sub>3</sub> molecules in both structures (see supplementary material).

The main differences of the hydrogen contacts in **1** and **1a** are given in Table VI. According to Taylor and Kennard<sup>34</sup> who have discussed crystallographic evidence for the existence of C–H $\cdots$ Cl contacts, the sum of the van der Waals radii for H and Cl is  $1.20 + 1.75 = 2.95$   $\text{\AA}$ . The contacts of 2.62–2.90  $\text{\AA}$  in the two structures may therefore be regarded as small but significant hydrogen-bonding contacts. Crystals of **1** and **1a** may be considered to be polymorphs of the same species on the basis of the crystallographic results. Clearly, these small packing differences cannot account for the blue-green difference in color, even without taking into consideration that this difference prevails in solution.

(33) Girolami, G. S.; Wilkinson, G.; Galas, M. R.; Thornton-Pett, M.; Hursthouse, M. B. *J. Chem. Soc., Dalton Trans.* **1985**, 1339.

(34) Taylor, R.; Kennard, O. *J. Am. Chem. Soc.* **1982**, *104*, 5063.

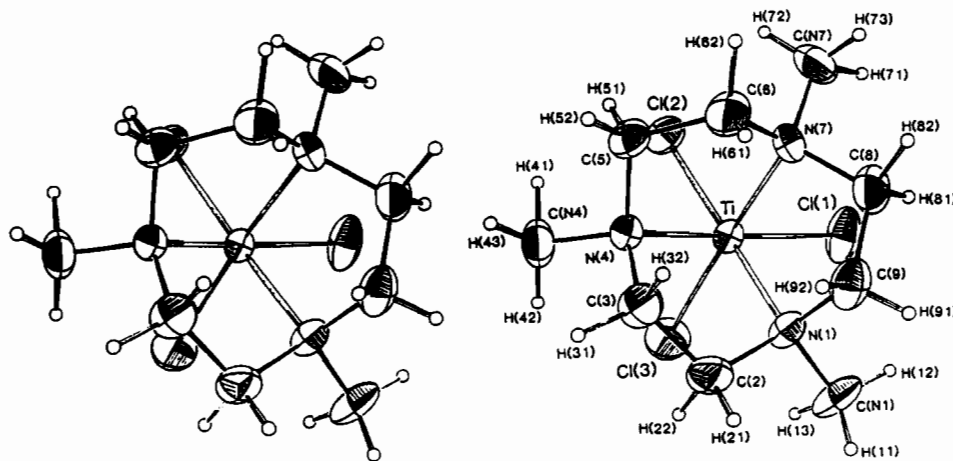


Figure 11. Stereoview and atom-labeling scheme of a neutral molecule in **1**. The same structure and labeling scheme are relevant for **1a**.

Table VI. Intermolecular C–H...Cl Contacts in **1** and **1a**

X–H...Y	X–H, Å	X...Y, Å	H...Y, Å	X–H...Y, deg	symm op
LTiCl <sub>3</sub> (Blue) ( <b>1</b> )					
C9–H92...Cl1	1.03 (4)	3.593 (4)	2.62 (4)	158 (3)	<i>x</i> , <i>l</i> + <i>y</i> , <i>z</i>
C3–H32...Cl1	1.07 (4)	3.676 (4)	2.88 (4)	126 (2)	<i>x</i> , <i>l</i> + <i>y</i> , <i>z</i>
C3–H32...Cl2	1.07 (4)	3.616 (4)	2.88 (4)	132 (2)	<i>x</i> , <i>l</i> + <i>y</i> , <i>z</i>
C5–H51...Cl2	0.99 (4)	3.635 (4)	3.03 (4)	121 (3)	– <i>x</i> , – <i>y</i> , – <i>z</i>
LTiCl <sub>3</sub> (Green) ( <b>1a</b> )					
C5–H51...Cl2	0.94 (4)	3.588 (4)	2.69 (4)	160 (3)	<i>x</i> , <i>l</i> + <i>y</i> , <i>z</i>
C2–H22...Cl2	0.94 (4)	3.688 (4)	3.03 (4)	128 (3)	<i>x</i> , <i>l</i> + <i>y</i> , <i>z</i>
C2–H22...Cl1	0.94 (4)	3.631 (4)	2.88 (4)	137 (3)	<i>x</i> , <i>l</i> + <i>y</i> , <i>z</i>
C9–H91...Cl1	1.03 (4)	3.659 (4)	2.90 (3)	131 (2)	1 – <i>x</i> , – <i>y</i> , – <i>z</i>

Table VII. Atomic Coordinates ( $\times 10^4$ ) and Equivalent Isotropic Displacement Parameters ( $\text{\AA}^2 \times 10^3$ ) for [LTiO(NCS)<sub>2</sub>] (**7**)

atom	<i>x</i>	<i>y</i>	<i>z</i>	<i>U</i> <sub>eq</sub>
Ti1	1973 (1)	249 (1)	0	33 (1)
O1	3143 (4)	1241 (2)	–2 (7)	54 (1)
S1	4545 (5)	–1553 (3)	–2254 (3)	78 (1)
S2	4581 (5)	–1574 (3)	2227 (3)	72 (1)
C11	3794 (9)	–909 (6)	–1491 (5)	38 (1)
C12	3819 (9)	–967 (7)	1507 (6)	51 (1)
N4	3276 (8)	–492 (7)	–946 (5)	53 (1)
N5	3247 (9)	–472 (6)	941 (6)	55 (1)
N1	–289 (8)	768 (5)	–856 (5)	44 (1)
N2	–264 (8)	730 (5)	876 (4)	40 (1)
N3	–359 (4)	–986 (2)	18 (7)	38 (1)
C1	–1561 (10)	1415 (6)	–414 (6)	87 (1)
C2	–1261 (11)	1488 (8)	420 (6)	107 (1)
C3	–1543 (10)	–25 (5)	1133 (6)	79 (1)
C4	–1131 (8)	–907 (4)	908 (4)	52 (1)
C5	–1852 (7)	–811 (4)	–577 (4)	52 (1)
C6	–1393 (11)	–25 (7)	–1183 (5)	90 (1)
C7	691 (11)	1189 (6)	–1568 (5)	73 (1)
C8	532 (9)	1231 (7)	1620 (5)	70 (1)
C9	477 (6)	–1931 (3)	–18 (9)	55 (1)

The Ti–Cl distances are within experimental error identical in **1** (average Ti–Cl 2.352 (1) Å) and **1a** (average Ti–Cl 2.351 (1) Å), as are the Ti–N bond lengths in **1** (average 2.256 (3) Å) and **1a** (average 2.272 (3) Å). The Ti–Cl distances agree well with other structures of the type Ti<sup>III</sup>Cl<sub>3</sub>A<sub>3</sub> and [TiCl<sub>2</sub>(B)<sub>4</sub>]<sup>+</sup>.<sup>35</sup> Again the crystal structure determinations of **1** and **1a** seem to indicate that **1** and **1a** consist of only LTiCl<sub>3</sub> molecules. However, careful inspection of the equivalent isotropic thermal parameters, *U*<sub>eq</sub>, of two of the Cl atoms in **1** and **1a** reveals that their values are ≈10% larger in **1a** than in **1** whereas values for the third Cl atom are identical in both structures. This might be interpreted as an indication that an oxygen atom of a 10% LTi(O)Cl<sub>2</sub> impurity is distributed on these two positions. In addition, it is noted, that the maximal residual electron density peak (0.56 e·Å<sup>–3</sup>) is observed

Table VIII. Selected Bond Lengths (Å) and Angles (deg) for [LTi(O)(NCS)<sub>2</sub>] (**7**)

Ti–O1	1.638 (3)	S1–C11	1.627 (9)
Ti–N4	2.075 (9)	S2–C12	1.547 (10)
Ti–N5	2.044 (9)	C11–N4	1.123 (12)
Ti–N1	2.241 (7)	C12–N5	1.225 (13)
Ti–N2	2.231 (6)		
Ti–N3	2.413 (3)		
O1–Ti–N4	102.3 (4)	O1–Ti–N2	95.5 (3)
O1–Ti–N5	102.2 (4)	N4–Ti–N2	159.9 (3)
N4–Ti–N5	95.6 (3)	N5–Ti–N2	89.7 (3)
O1–Ti–N1	94.3 (3)	N1–Ti–N2	77.5 (3)
N4–Ti–N1	91.7 (3)	O1–Ti–N3	167.2 (1)
N5–Ti–N1	160.0 (3)	N4–Ti–N3	86.7 (3)
N5–Ti–N3	85.8 (3)	N1–Ti–N3	76.1 (2)
N2–Ti–N3	74.4 (3)	S1–C11–N4	177.5 (8)
		S2–C12–N5	178.5 (5)

at a 1.59-Å distance from the titanium ion in **1a**. No such residual electron density is observed in the vicinity of the titanium ion in the structure of **1**.

Atom coordinates for [LTi(O)(NCS)<sub>2</sub>] (**7**) are listed in Table VII; Table VIII summarizes important bond lengths and angles. Crystals of **7** consist of neutral molecules of [LTi(O)(NCS)<sub>2</sub>], of which Figure 12 shows the structure. **7** is the first structurally characterized octahedral titanil complex. The Ti=O bond length of 1.638 (3) Å is short and indicates considerable double-bond character. In five-coordinate titanil porphyrin complexes this bond is 1.62 Å<sup>14–16</sup> whereas in the seven-coordinate complex [TiO(CO<sub>3</sub>)<sub>3</sub>]<sup>4–</sup> the Ti=O bond is quite long at 1.680 (2) Å,<sup>19</sup> which is a consequence of two relatively strong hydrogen-bonding contacts to the Ti=O group. The three Ti(IV)–N<sub>amine</sub> distances in **7** are not equivalent. Ti–N3 in the trans position to the Ti=O group is longer by 0.18 Å than the average of the two Ti–N<sub>amine</sub> bonds at 2.236 (10) Å in the cis position. This is a clear manifestation of a strong structural trans influence of the Ti=O group.<sup>36</sup>

The thiocyanato ligands are N-bound; the corresponding average Ti–N<sub>NCS</sub> bond length of 2.044 (10) Å is considerably

(35) (a) Drew, M. G. B.; Hutton, J. A. *J. Chem. Soc., Dalton Trans.* **1978**, 1176. (b) Hughes, D. L.; Leigh, G. J.; Walker, D. G. *J. Chem. Soc., Dalton Trans.* **1988**, 5513. (c) Drew, M. G. B.; Collins, R. K. *Inorg. Nucl. Chem. Lett.* **1972**, 8, 975.

(36) Nugent, W. A.; Mayer, J. M. *Metal-Ligand Multiple Bonds*; Wiley: New York, 1988.

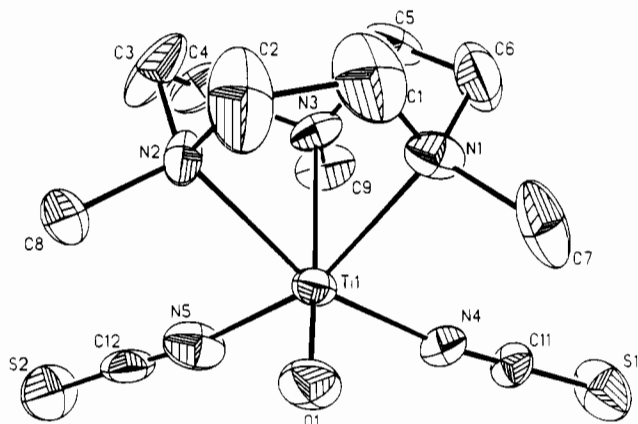


Figure 12. Structure and atom-labeling scheme of a neutral molecule in 7.

Table IX. Atomic Coordinates ( $\times 10^4$ ) and Equivalent Isotropic Displacement Coefficients ( $\text{\AA}^2 \times 10^3$ ) for  $[\text{LTi}(\text{OCH}_3)_2\text{Br}_2](\text{ClO}_4)$  (8)

atom	x	y	z	$U_{\text{eq}}^a$
Br1	942 (1)	935 (2)	6661 (2)	107 (1)
Ti	1630 (2)	2500	5566 (3)	62 (1)
N1	3129 (12)	2500	6544 (16)	86 (8)
N2	2614 (8)	1299 (11)	4660 (10)	73 (5)
O1	663 (8)	2500	4623 (10)	82 (6)
C1	2981 (18)	2500	7730 (16)	114 (12)
C2	3705 (13)	1457 (18)	6222 (15)	149 (11)
C3	3504 (14)	895 (16)	5264 (14)	125 (10)
C4	3046 (13)	1883 (15)	3722 (12)	151 (10)
C5	2033 (14)	297 (18)	4292 (15)	140 (10)
C6	-238 (14)	2500	3976 (17)	107 (11)
C1	1409 (5)	2500	1018 (6)	95 (3)
O2	933 (11)	1577 (11)	1509 (10)	168 (7)
O3	1171 (15)	2500	4 (16)	185 (12)
O4	2386 (12)	2500	1236 (15)	232 (17)

<sup>a</sup> Equivalent isotropic  $U$  defined as one-third of the trace of the orthogonalized  $U_{ij}$  tensor.

Table X. Selected Bond Lengths ( $\text{\AA}$ ) and Angles (deg) for  $[\text{LTi}(\text{OCH}_3)_2\text{Br}_2](\text{ClO}_4)$  (8)

Br1-Ti	2.451 (3)	Ti-N1	2.287 (17)
N2-Ti	2.203 (12)	Ti-O1	1.723 (12)
Br1-Ti-N1	89.7 (3)	Br1-Ti-N2	91.9 (3)
N1-Ti-N2	78.6 (5)	Br1-Ti-O1	97.7 (3)
N1-Ti-O1	168.9 (6)	N2-Ti-O1	92.9 (4)
Br1-Ti-Br1a	95.6 (1)	N2-Ti-Br1a	166.1 (3)
N2-Ti-N2a	78.5 (6)	Ti-O1-C6	171.4 (12)

shorter than the cis Ti-N<sub>amine</sub> bonds ( $\Delta = 0.19 \text{\AA}$ ). The NCS- ligands are nearly linearly coordinated to Ti(IV); The Ti-N<sub>NCS</sub> bonds display some multiple-bond character.

Atom coordinates for  $[\text{LTi}(\text{OCH}_3)_2\text{Br}_2](\text{ClO}_4)$  (8) are listed in Table IX; Table X summarizes selected bond lengths and angles. Crystals of 8 consist of the monocation  $[\text{LTi}(\text{OCH}_3)_2\text{Br}_2]^+$  and perchlorate anions. The Ti(IV) center is in a pseudooctahedral environment consisting of a facially bound macrocyclic amine, two bromo ligands, and a coordinated methoxy group (Figure 13). The cation possesses a crystallographic mirror plane; atoms Ti1, O1, C6, N1, and C1 lie on this plane. Site symmetry  $m$  is not compatible with the ( $\lambda\lambda\lambda$ ) or ( $\delta\delta\delta$ ) configuration at the three five-membered chelate rings  $\text{Ti-N-C-C-N}$  and, therefore, the methylene carbon atoms are disordered, as is borne out by physically meaningless, large anisotropic thermal parameters for C2, C3, and C4 and short C-C bond distances. Attempts to model this disorder by a split-atom model for methylene carbon atoms failed.

The Ti(IV)-Br1 bond length of 2.451 (3)  $\text{\AA}$  is as in other

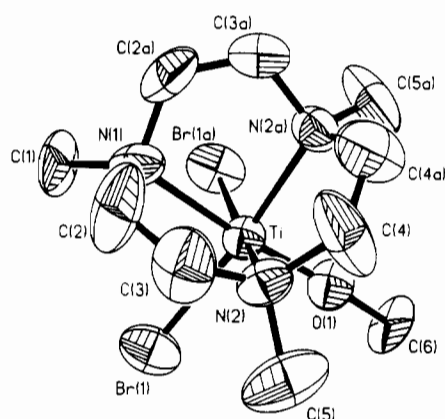


Figure 13. Structure and atom-labeling scheme of the monocation in 8.

Table XI. Atomic Coordinates ( $\times 10^4$ ) and Equivalent Isotropic Displacement Parameters ( $\text{\AA}^2 \times 10^3$ ) for  $[\text{L}_2\text{Ti}_2(\text{O})_2\text{F}_2(\mu\text{-F})](\text{PF}_6)$  (13)

atom	x	y	z	$U_{\text{eq}}^a$
Ti1	184 (1)	4871 (1)	8656 (1)	39 (1)
F1	0	5000	10000	55 (2)
F2	1007 (5)	2371 (4)	8759 (2)	67 (1)
O1	-2200 (4)	5497 (5)	8458 (2)	53 (1)
N1	917 (6)	5212 (6)	6936 (3)	57 (2)
N2	3214 (5)	4850 (5)	8404 (3)	48 (1)
N3	-8 (5)	7988 (5)	8089 (3)	46 (1)
C1	2945 (10)	4377 (14)	6754 (6)	120 (5)
C2	4060 (9)	4459 (14)	7402 (5)	122 (5)
C3	3226 (9)	6701 (9)	8469 (7)	107 (4)
C4	1750 (8)	8263 (9)	8198 (7)	97 (4)
C5	-360 (12)	8513 (9)	7006 (4)	99 (3)
C6	313 (15)	7187 (10)	6428 (5)	118 (5)
C7	7 (10)	4115 (10)	6567 (4)	86 (3)
C8	4288 (6)	3391 (7)	9200 (4)	58 (2)
C9	-1543 (7)	9181 (7)	8668 (4)	62 (2)
P1	5000	0	5000	58 (1)
F11	4471 (9)	2167 (6)	4630 (4)	161 (3)
F12	4916 (9)	19 (8)	6133 (4)	167 (4)
F13	2961 (7)	187 (10)	5209 (5)	210 (4)

<sup>a</sup> Equivalent isotropic  $U$  defined as one-third of the trace of the orthogonalized  $U_{ij}$  tensor.

bromotitanium(IV) complexes.<sup>37</sup> The Ti-N<sub>amine</sub> distance 2.203 (12)  $\text{\AA}$  in the trans position relative to Br- ligands represents a normal Ti-N<sub>amine</sub> bond which is not affected by a trans influence. In contrast, the Ti-N1 bond is longer by 0.08  $\text{\AA}$ , indicating a weak but significant trans influence of the methoxy group. The Ti-O1 distance of 1.723 (12)  $\text{\AA}$  is short and probably indicates some double-bond character. The Ti-O1-C6 bond angle is 171.4°; thus nearly linear coordination of the sterically undemanding methoxy group is observed. Ti-O distances in terminal alkoxytitanium(IV) complexes are typically in the range 1.70–1.80  $\text{\AA}$ .<sup>3</sup>

Atom coordinates for  $[\text{L}_2\text{Ti}_2\text{F}_2(\text{O})_2(\mu\text{-F})](\text{PF}_6)$  (13) are given in Table XI; Table XII summarizes bond lengths and angles. Figure 14 shows the structure and atom-labeling scheme for the dinuclear cation in 13. The terminal ligands F2 and O1 are not discernible by X-ray crystallography; their respective assignments have been made for the sake of clarity. The distances Ti-F(2) of 1.784 (3)  $\text{\AA}$  and Ti-O1 of 1.778 (3)  $\text{\AA}$  appear to be equidistant but they reflect this disorder (Figure 10). In octahedral titanium(IV) complexes the average Ti-F<sub>i</sub> distance is 1.91 (1)  $\text{\AA}$ <sup>38</sup> whereas the Ti=O length is 1.64 (1)  $\text{\AA}$ . The average of these

(37) (a) Palacios, F.; Royo, P.; Serrano, R.; Balcazar, J. L.; Fouseca, I.; Florencio, F. *J. Organomet. Chem.* **1989**, 375, 51. (b) Lecomte, C.; Protas, J.; Marchon, J.-C.; Nakjima, M. *Acta Crystallogr.* **1978**, B34, 2856.

(38) Schmidt, R.; Pausewang, G. *Z. Anorg. Allg. Chem.* **1988**, 559, 135.

(39) Schreiber, P.; Wieghardt, K.; Nuber, B.; Weiss, J. *Z. Anorg. Allg. Chem.* **1990**, 587, 174.

(40) Desroches, P. J.; Enemark, J. H. Work in progress.

**Table XII.** Selected Bond Lengths (Å) and Angles (deg) for  $[\text{L}_2\text{Ti}_2\text{O}_2\text{F}_2(\mu\text{-F})](\text{PF}_6)$  (**13**)<sup>a</sup>

Ti1-F1	1.884 (1)	Ti1-N1	2.286 (4)
Ti2-F2	1.784 (3)	Ti1-N2	2.284 (4)
Ti1-O1	1.778 (3)	Ti1-N3	2.283 (4)
F2-Ti1-F1	100.7 (1)	N2-Ti1-O1	160.1 (1)
O1-Ti1-F1	101.5 (1)	N2-Ti1-N1	75.7 (2)
O1-Ti1-F2	103.5 (2)	N3-Ti1-F1	92.7 (1)
N1-Ti1-F1	164.5 (2)	N3-Ti1-F2	159.7 (1)
N1-Ti1-F2	88.2 (1)	N3-Ti1-O1	88.5 (2)
N1-Ti1-O1	88.6 (2)	N3-Ti1-N1	75.6 (2)
N2-Ti1-F1	91.7 (1)	N3-Ti1-N2	75.9 (1)
N2-Ti1-F2	88.4 (2)	Ti1-F1-Ti1a	180.0

<sup>a</sup> Atoms O1 and F2 are crystallographically not discernible; their positions are disordered (O/F); see text.

two values is 1.775 Å in agreement with the above Ti—F/O distances. As we have shown above, the presence of one bridging fluoride (F1), two terminal fluorides, and two terminal oxo ligands per dinuclear cation is established unambiguously by infrared and <sup>17</sup>F NMR spectroscopy. The Ti—F—Ti' structural unit is linear and the Ti—F<sub>b</sub> distance of 1.884 (1) Å is shorter than in edge-sharing bis(μ-fluoro)ditanium(IV) complexes,<sup>38</sup> indicating small Ti—F double-bond character.

A further indication for the disorder in **13** is the apparent lack of a trans influence on the Ti—N bond trans to the terminal oxo group. All three Ti—N distances appear to be identical within experimental error due to the averaging effect of the packing of structures A, B, and C (Figure 10) in crystals of **13**.

## Discussion

In this section we discuss the most salient features of this investigation. First we want to emphasize the implications of the chemistry and the X-ray crystallography of the blue and green forms of  $[\text{LTiCl}_3]$  with respect to the problem or experimental verification of distortional isomerism<sup>5</sup> (bond stretch isomerism<sup>9</sup>).

This term was originally coined by Butcher and Chatt<sup>5</sup> for the observation that *cis,mer*- $\text{MoOCl}_2(\text{PMe}_2\text{Ph})_3$  was obtained in a blue and a green form which displayed significantly differing Mo=O bond lengths in the solid state as the only remarkable structural difference. Parkin et al.<sup>11</sup> and Enemark et al.<sup>12</sup> have recently demonstrated that this is an artifact. The green form is a mixture of  $\text{MoOCl}_2(\text{PMe}_2\text{Ph})_3$  (blue) and *mer*- $\text{MoCl}_3(\text{PMe}_2\text{Ph})_3$  (yellow) which cocrystallize to yield green crystals. It was shown that adding increasing amounts of yellow *mer*- $\text{MoCl}_3(\text{PMe}_2\text{Ph})_3$  to blue  $\text{MoOCl}_2(\text{PMe}_2\text{Ph})_3$  affords green crystals with a continuum of apparently increasing Mo=O bond lengths.<sup>11</sup> X-ray structure determinations on *compositionally disordered crystals*<sup>12</sup> produced the differences of Mo=O bond lengths.

A second, still unresolved, example of this kind has been reported for  $[\text{LWOC}_2](\text{PF}_6)$  where also blue and green crystals have been obtained.<sup>6a</sup> Again, an apparent difference in W=O bond distances was reported. Both kinds of crystals dissolve in dry acetonitrile with retention of the blue or green color. The electronic spectra of both species show that the green form exhibits a very prominent CT band at 419 nm which is not present in the blue form. Both species exhibit a weak d—d transition at 693 nm ( $\epsilon = 40 \text{ L}\cdot\text{mol}^{-1}\cdot\text{cm}^{-1}$ ). It was reported that the CT band vanishes immediately when a few drops of water were added to a green acetonitrile solution, yielding the spectrum of the blue form. At this time it has *not* been established experimentally that the CT and the d—d absorption maxima of the green form belong to the

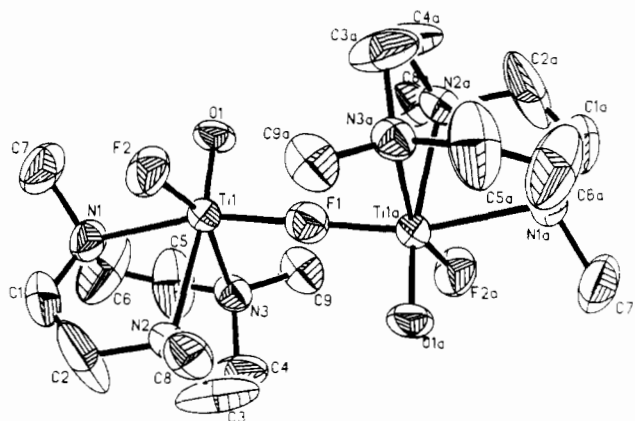


**Figure 14.** Structure and atom-labeling scheme of the dinuclear cation in **13**. F2 and O1 are disordered (see text).

same species. In particular, the intensity ratio of the two maxima of different preparations of the green form has not been measured.

It is rather amazing that at least the solution chemistry of green  $\text{LTiCl}_3$  is very similar to that of *green*  $[\text{LWOC}_2](\text{PF}_6)$ . It clearly indicates that *green*  $[\text{LWOC}_2](\text{PF}_6)$  could also be a mixture of two species, namely blue  $[\text{LWOC}_2](\text{PF}_6)$  and *yellow*  $[\text{LWO}_2\text{Cl}](\text{PF}_6)$ , the oxidized form of the tungsten(V) complex.  $[\text{LWO}_2\text{Cl}]^+$  is unstable with respect to hydrolysis with excess water, yielding the colorless dinuclear species  $[\text{L}_2\text{W}_2\text{O}_4(\mu\text{-O})]^{2+}$ .<sup>39</sup> Experiments to verify this hypothesis are under way.<sup>40</sup>

From spectroscopic data (infrared and electronic absorption spectroscopy) we have been able to show unambiguously that *green*  $[\text{LTiCl}_3]$  (**1a**) is compositionally disordered; it contains an estimated 10% of presumably *yellow*  $\text{LTiOCl}_2$ . Rather surprisingly, this impurity did not show up very clearly in the X-ray structure determination of **1a**. The structure determination of **1a** is of excellent quality considering the fact that all hydrogen atoms were located and refined. Only weak hints which support the spectroscopic results of an impurity are obtained by X-ray crystallography. The message here is that X-ray crystallography is not a sensitive method to verify the purity of a compound. These results should be taken as a further caveat for the notion that recrystallization is always a purifying process.<sup>12</sup>

The second important result of this study is the successful synthesis of complexes **7**, **12**, and **13**, all of which contain octahedral titanium(IV) ions and a terminal oxo ligand. The Ti=O group has been identified by vibrational spectroscopy and X-ray crystallography. **7** represents the first genuine, crystallographically characterized example for a mononuclear octahedral titanyl complex. It is noted that  $\text{TiO}(\text{edtaH}_2)\cdot(\text{H}_2\text{O})$  is probably also six-coordinate.<sup>41</sup> It exhibits a Ti=O stretching frequency at  $950 \text{ cm}^{-1}$ . Complexes **12** and **13** have structural motifs quite commonly observed in vanadium(V)<sup>31</sup> chemistry. They represent the first examples of this type in titanium(IV) coordination chemistry.

**Acknowledgment.** We thank Dr. P. J. Desroches and Professor J. H. Enemark for helpful discussions. Financial support of this work by the Fonds der Chemischen Industrie is gratefully acknowledged.

**Supplementary Material Available:** Packing diagrams for **1** and **1a** and a perspective view of the molecule in **1a**, tables listing details of data collection, structure solution, and refinement, bond distances and angles, anisotropic thermal parameters of all non-hydrogen atoms, and positional parameters of hydrogen atoms (found and refined in **1** and **1a**, calculated for **7**, **8**, and **13** for **1**, **1a**, **7**, **8**, and **13**, and tables giving non-hydrogen positional *q* parameters for **1** and **1a** (29 pages); listings of *F<sub>o</sub>* and *F<sub>c</sub>* (58 pages). Ordering information is given on any current masthead page.

(41) Kristine, F. J.; Shepherd, R. E.; Siddiqui, S. *Inorg. Chem.* **1981**, *20*, 2571.